



**REPORT**

**Updated Summary of Hydrogeology Existing Conditions**  
*Meliadine Extension*

Submitted to:

**Agnico Eagle Mines Limited**

Submitted by:

**Golder Associates Ltd.**

Suite 200 - 2920 Virtual Way, Vancouver, British Columbia, V5M 0C4, Canada

+1 604 296 4200

Reference No. 22513890-942-R-Rev0-2000

14 December 2022

A large, solid red abstract shape that resembles a stylized mountain peak or a large arrow pointing upwards and to the right. It occupies the lower half of the page, starting from the left margin and extending towards the right edge.

## Distribution List

Electronic Copy - Agnico Eagle Mines Limited

Electronic Copy - Golder Associates Ltd

Electronic Copy - Nuqsana Golder

# Table of Contents

<b>1.0 INTRODUCTION .....</b>	<b>1</b>
<b>2.0 HYDROGEOLOGY STUDY AREA.....</b>	<b>1</b>
<b>3.0 DATA REVIEW AND ANALYSIS .....</b>	<b>3</b>
3.1 Lake Elevations and Bathymetry Data.....	3
3.2 Structural Geology Review.....	3
3.3 Summary of Hydrogeological Testing .....	7
3.3.1 2009 and 2011 Tiriganiaq Testing Program .....	7
3.3.2 2015 Tiriganiaq Testing Program.....	10
3.3.3 2019-2020 Tiriganiaq Testing Program .....	13
3.3.4 2020 Discovery Testing Program.....	16
3.3.5 2021 Geotechnical Site Investigation .....	19
3.3.6 2021 Wesmeg Testing Program .....	19
3.3.7 2021 Discovery Testing .....	19
3.3.8 2021 Pump, Wesmeg, Fzone, and Lake B5 Testing Programs .....	22
3.4 Groundwater Sampling .....	26
3.4.1 Data Collection.....	26
3.4.2 Groundwater Salinity Profile .....	27
3.5 Permafrost Conditions.....	27
3.5.1 Depth to Permafrost and Lakes with Open Talik .....	27
3.5.2 Cryopeg Depth.....	31
3.6 Tiriganiaq Groundwater Inflow Monitoring .....	31
3.7 Hydraulic Head Monitoring.....	33
3.7.1 Tiriganiaq Area.....	33
3.7.2 Discovery Area.....	34
<b>4.0 CONCEPTUAL HYDROGEOLOGICAL MODEL .....</b>	<b>40</b>
4.1 Permafrost Depth.....	40

4.2	Hydrostratigraphy.....	40
4.2.1	Geologic Context .....	40
4.2.2	Bedrock Hydrostratigraphy .....	43
4.2.3	Enhanced Permeability Zones Associated with Faults .....	45
4.2.4	Estimated Hydraulic Properties.....	46
4.3	Conceptual Groundwater Flow – Pre-Mining .....	49
4.4	Conceptual Groundwater Flow – Existing Conditions.....	51
<b>REFERENCES .....</b>		<b>53</b>

## TABLES

Table 1: Summary of Available Hydraulic Testing Results – 2014 FEIS .....	8
Table 2: Summary of Packer Tests – 2015 Underground Program .....	11
Table 3: Summary of Flow Recession Pumping Tests – 2015 Underground Program .....	12
Table 4: Summary of Injection Trial Results in TIS-200-022 – 2015 Underground Program.....	12
Table 5: Summary of Estimated Hydraulic Conductivity and Diffusivity Values from Long Term Recession Test at WH350-157-D1 .....	15
Table 6: Summary of Hydraulic Test Results Near Discovery Underground – Fall of 2020 .....	17
Table 7: Summary of Hydraulic Tests Results from the 2021 Geotechnical Site Investigation .....	20
Table 8: Summary of Hydraulic Tests Results from the 2021 Wesmeg Underground Testing Program.....	20
Table 9: Summary of Hydraulic Tests Results Near Discovery Underground – Fall 2021 .....	21
Table 10: Summary of Hydraulic Tests Results in 2020-2021 Underground Program .....	24
Table 11: Thermistor Summary .....	29
Table 12: Estimated Freshwater Heads, Flow Directions and Gradients – M11-1257 and Lake B7 .....	33
Table 13: Estimated Freshwater Heads, Flow Directions and Gradients - M11-1257 and Lake B5.....	34
Table 14: Estimated Freshwater Hydraulic Heads and Vertical Hydraulic Gradients .....	35
Table 15: Estimated Hydraulic Properties - Competent Bedrock.....	47
Table 16: Estimated Hydraulic Properties – Enhanced Permeability Zones.....	48



## FIGURES

Figure 1: Hydrogeology Study Area .....	2
Figure 2: Structures of Enhanced Permeability – Main Area and Tiriganiaq-Wolf.....	5
Figure 3: Structures of Enhanced Permeability – Discovery Area .....	6
Figure 4: Borehole Locations for Hydraulic Testing and Groundwater Sampling – Main Area.....	9
Figure 5: Borehole Locations for Hydraulic Testing and Groundwater Sampling – KMS Corridor .....	14
Figure 6: Groundwater Salinity Profile with Depth.....	28
Figure 7: Groundwater Inflow Measurements for the Tiriganiaq Underground .....	32
Figure 8: Pressure Monitoring Data – Tiriganiaq Underground – Part 1.....	36
Figure 9: Pressure Monitoring Data – Tiriganiaq Underground – Part 2.....	37
Figure 10: Pressure Monitoring Data – Tiriganiaq Underground – Part 3.....	38
Figure 11: Pressure Monitoring Data – Tiriganiaq Underground – Part 4.....	39
Figure 12: Regional Geology .....	41
Figure 13: Summary of Hydraulic Conductivity Results .....	44
Figure 14: Conceptual Permafrost and Groundwater Flow Model Baseline Conditions .....	50

## APPENDICES

### APPENDIX A

Location of Thermal Model Cross-Sections

## 1.0 INTRODUCTION

Agnico Eagle Mines Limited (Agnico Eagle) is proposing to expand the development at the Meliadine Gold Project (herein referred to as the Meliadine Extension or the Project), located approximately 25 km north from Rankin Inlet and 80 km southwest from Chesterfield Inlet in the Kivalliq Region of Nunavut. The Project includes open-pits and the Tiriganiaq underground development assessed through the 2014 FEIS (Agnico Eagle 2014a) plus new underground developments.

In 2021, Golder Associates Ltd., a member of WSP (WSP Golder) documented a summary of hydrogeology existing conditions for the Project to provide the foundation for a qualitative and quantitative assessment of the Project with respect to groundwater (Golder 2021f). Since completion of this work, supplemental hydrogeological data has been collected to enhance the understanding of hydrogeological conditions. This report presents a summary of the supplemental data collection and an updated summary of the hydrogeology existing conditions for the Project based on the inclusion of that data.

The objective of the updated hydrogeology existing conditions report is to characterize the groundwater conditions in areas that will be potentially influenced by Mine development. The available data on existing conditions will be used to inform groundwater modelling, supplemental effects assessment (if required), water management plans and future groundwater effects monitoring.

## 2.0 HYDROGEOLOGY STUDY AREA

The hydrogeology study area is presented on Figure 1, relative to the existing and proposed underground developments and open pits. The study area is consistent with the regional study area from the 2014 FEIS (Agnico Eagle 2014a) and includes major lakes with interpreted open taliks, the largest of which is Meliadine Lake present to the east, north and west of the existing and proposed developments.



### 3.0 DATA REVIEW AND ANALYSIS

Section 3.0 of this report presents an updated summary of the hydrogeological data used to define the hydrogeology existing conditions for the Project. Supplemental data collected since the previous summary of existing conditions (Golder 2021f) includes:

- 2021 packer testing near Lake B5 and near the proposed Discovery, Wesmeg, Pump and Fzone undergrounds (Sections 3.3.5 to 3.3.8).
- Supplemental groundwater sampling at Westbay well M20-3071 and the Tiriganiaq underground (Section 3.4).
- Updated thermal modelling to define permafrost conditions (Section 3.5).
- Supplemental groundwater inflow monitoring at the existing Tiriganiaq underground (Section 3.6).
- Hydraulic head monitoring in Westbay wells and select piezometers near the existing Tiriganiaq underground (Section 3.7).

#### 3.1 Lake Elevations and Bathymetry Data

Approximate elevations of lakes near the Project were obtained from the local topographic survey data, as provided by Agnico Eagle. Where local survey data were not available, approximate lake elevations were obtained from the National Topographic System (NTS) map sheets published by the Government of Canada.

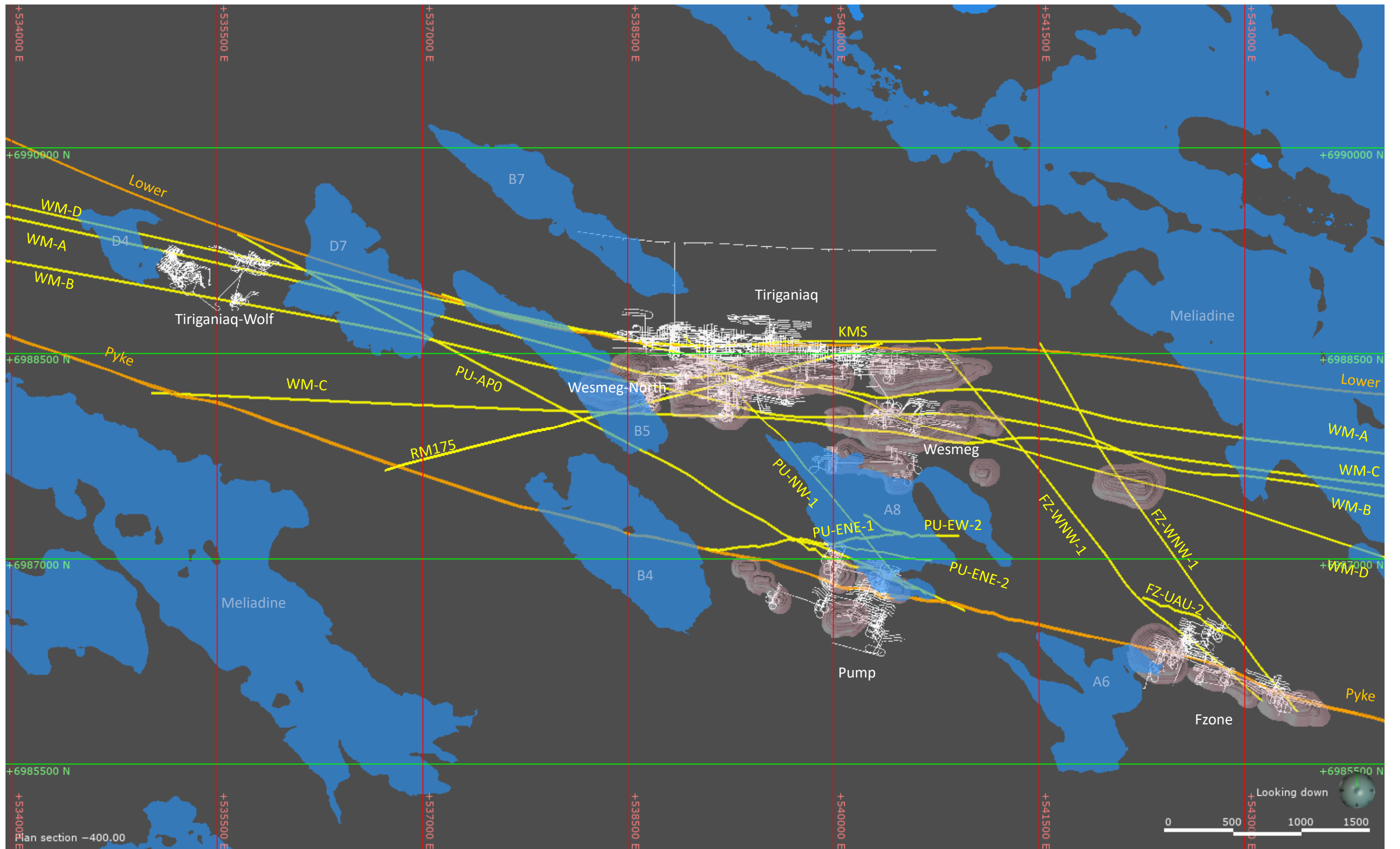
As documented in the 2014 FEIS (Agnico Eagle 2014a), bathymetry data for lakes near the existing and proposed developments were obtained from data collected during field programs in 1997 and 1998 (RL&L 1999) and in 2001 (SD 7-1 2009 Aquatic Synthesis Report and DS 7-2 2011 Aquatics Baseline from the 2014 FEIS [Agnico Eagle 2014a]) and provided to Golder by Agnico Eagle.

#### 3.2 Structural Geology Review

In the 2014 FEIS, three regional structures were considered in hydrogeological assessment (Lower Fault, Pyke Fault and North Fault). In support of the Project, Agnico Eagle completed a review of the structures near the proposed underground developments through examination of more recent drilling data, magnetic surveys breaks and interpretation of surficial lineaments. The objective of the review was to identify significant structures of potential enhanced permeability that may intersect the existing and proposed underground developments and be present within unfrozen bedrock. This review led to the identification of 17 faults that have been incorporated into the conceptual hydrostratigraphy, in addition to the 3 regional faults (Lower Fault, Pyke Fault and North Fault) that were previously considered in the 2014 FEIS.

The location of the faults identified by Agnico Eagle are presented on Figure 2 and Figure 3. The additional structures are generally located between the Lower Fault and Pyke Fault within the Mafic Volcanic Rock formations and range in thickness between 2 and 6 m based on information provided by Agnico Eagle. An exception is the KMS corridor, which is a wider zone of poor rock quality that is generally located between the KMS fault and Lower Fault.

In the area of the existing Tiriganiaq underground, there is a higher confidence in the structural interpretation and their presence as enhanced permeability features, particularly the RM175 and the KMS Fault Corridor. At the other underground developments, less testing has been done to verify that the identified structures have enhanced permeability, with the collection of data in these areas being a priority for the 2021 field programs (Section 3.3.5 to 3.3.8). Given the limited site-specific data, the structures have been conservatively assumed to have enhanced permeability relative to the surrounding bedrock, to extend several kilometres away from the underground development and to extend to a depth of approximately one kilometre (-1025 m elevation). The lateral extent of the KMS corridor is somewhat uncertain and was interpreted to encompass a zone of poor rock quality between the KMS Fault and Lower Fault. Based on input from Agnico Eagle geologists, a permeable 'skin' has been assumed along the lower fault of 15 to 20 m width to account for the potential extension of this corridor to the east and west.



**LEGEND**

- Inferred Lake with Open Talik
  - Regional Fault
  - Supplemental Faults Based on 2020 Agnico Eagle Review
- Fault traces are shown for an elevation of -400 masl.

CLIENT



CONSULTANT



YYYY-MM-DD	2021-05-25
PREPARED	HG
DESIGNED	HG
REVIEWED	JL
APPROVED	DC

PROJECT

AGNICO EAGLE MINES LIMITED  
MELIADINE EXTENSION  
NUNAVUT

TITLE

**STRUCTURES OF ENHANCED PERMEABILITY – MAIN  
AREA AND WOLF**

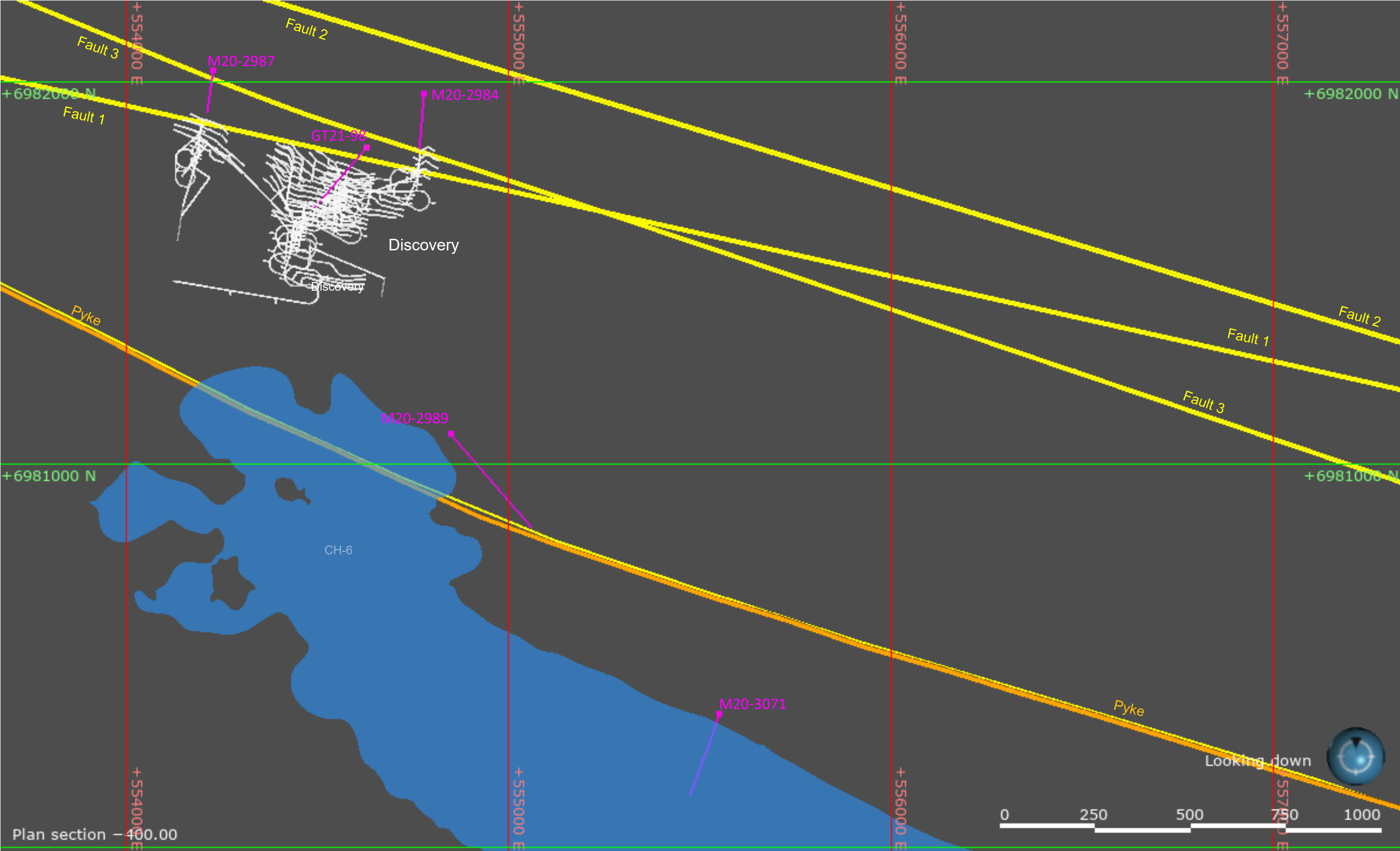
PROJECT NO.  
22513890

PHASE  
2000

REV.  
0

FIGURE  
2





**LEGEND**

- Inferred Lake with Open Talik
- Regional Fault
- Supplemental Faults Based on 2020 Agnico Eagle Review
- Borehole Collar / Borehole Trace

Fault traces are shown for an elevation of -400 masl.

CLIENT



CONSULTANT



YYYY-MM-DD	2021-05-25
PREPARED	HG
DESIGNED	HG
REVIEWED	JL
APPROVED	DC

PROJECT

AGNICO EAGLE MINES LIMITED  
MELIADINE EXTENSION  
NUNAVUT

TITLE

**STRUCTURES OF ENHANCED PERMEABILITY –  
DISCOVERY AREA**

PROJECT NO.  
22513890

PHASE  
2000

REV.  
0

FIGURE  
3

### 3.3 Summary of Hydrogeological Testing

#### 3.3.1 2009 and 2011 Tiriganiaq Testing Program

Hydraulic test data from two field programs (one in 2009 and one in 2011) was available at the time of the 2014 FEIS (Agnico Eagle 2014a). A summary of these hydraulic testing results is summarized in Table 1 and the location of the boreholes tested are presented on Figure 4.

In 2009, three-single well response tests were conducted in 2 boreholes (Golder 2009; Golder 2011). Two of these tests were conducted in borehole GT09-19 within the talik of Lake B7 at vertical depths of about 40 metres below ground surface (mbgs) and 100 mbgs. The third test was conducted in borehole M09-860 from about 420 to 560 mbgs.

In 2011, seven single-well response tests were conducted at borehole M11-1257, located near Lake B5 to the west of Tiriganiaq Underground (Golder 2011). The first two tests were conducted using a packer at depths of 459 to 601 mbgs and 596 to 632 mbgs. Tests 3 through 7 at this location were conducted after the installation of a Westbay system in the borehole and were conducted in intervals 2 (602 to 613 mbgs), 2A (615 to 623 mbgs), 3 (574 to 585 mbgs), 4 (519 to 530 mbgs) and 5 (449 to 461 mbgs) respectively. The transmissivity and bulk hydraulic conductivity in the Westbay intervals were estimated from the pressure response collected by transducers within the sampling cylinders of the Westbay system.

In each of boreholes M09-860 and M11-1257, a single-well response test was conducted over an interval in deep bedrock that included the Lower Fault Zone. At M09-860 this included Test#1, which had an estimated transmissivity of  $5 \times 10^{-7} \text{ m}^2/\text{s}$ . Assuming a five-metre-wide fault, this would indicate a Lower Fault hydraulic conductivity of  $1 \times 10^{-7} \text{ m/s}$ . At M11-1257 this included Test #2, which had an estimated transmissivity of  $1 \times 10^{-7} \text{ m}^2/\text{s}$ . assuming a five-metre-wide fault, this would indicate a Lower Fault hydraulic conductivity of  $5 \times 10^{-8} \text{ m/s}$ . The hydraulic conductivity estimates of the bulk bedrock excluding the Lower Fault Zone ranged from  $5 \times 10^{-10}$  to  $7 \times 10^{-9} \text{ m/s}$ .

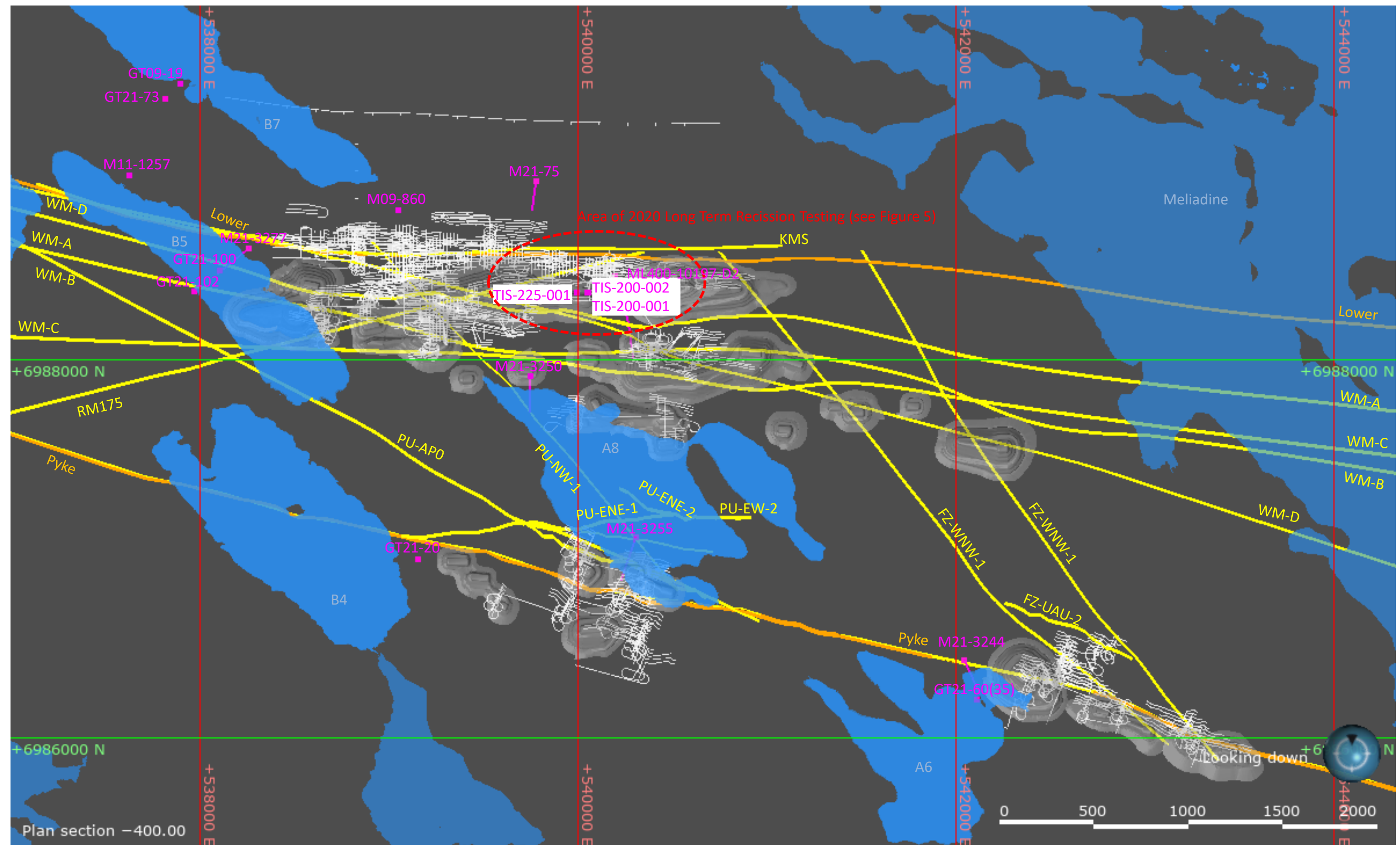


**Table 1: Summary of Available Hydraulic Testing Results – 2014 FEIS**

Borehole	Test #	Interval Top (mbgs)	Interval Bottom (mbgs)	Interval Midpoint (mbgs)	West Bay Interval	Transmissivity (m <sup>2</sup> /s)	Hydraulic Conductivity <sup>1</sup> (m/s)	Geology
GT09-19	1	27	56	42	-	$1 \times 10^{-7}$	$3 \times 10^{-9}$	Sam Formation
GT09-19	2	54	153	104	-	$2 \times 10^{-7}$	$2 \times 10^{-9}$	Sam Formation
M09-860	1	424	563	494	-	$5 \times 10^{-7}$	$4 \times 10^{-9}$	Sam Formation, Upper Oxide Formation, Wesmeg Formation, Lower Fault
M11-1257	7	449	461	455	Interval 5	$3 \times 10^{-8}$	$2 \times 10^{-9}$	Sam Formation
M11-1257	6	519	530	525	Interval 4	$6 \times 10^{-8}$	$5 \times 10^{-9}$	Sam Formation
M11-1257	5	574	585	580	Interval 3	$8 \times 10^{-8}$	$7 \times 10^{-9}$	Upper Oxide
M11-1257	4	615	623	619	Interval 2A	$1 \times 10^{-8}$	$1 \times 10^{-9}$	Wesmeg/Lower Fault
M11-1257	3	602	613	608	Interval 2	$2 \times 10^{-8}$	$2 \times 10^{-9}$	Tiriganiaq
M11-1257	2	596	632	614	-	$1 \times 10^{-7}$	$3 \times 10^{-9}$	Upper Oxide, Tiriganiaq, Wesmeg, Lower Fault
M11-1257	1	459	601	530	-	$7 \times 10^{-8}$	$5 \times 10^{-10}$	Sam Formation and Upper Oxide


1) Calculated based on estimated transmissivity and test interval length.

mbgs = metres below ground surface; m<sup>2</sup>/s = square metres per second; m/s = metres per second.



- LEGEND**
- Inferred Lake with Open Talik
  - Regional Fault
  - Supplemental Faults Based on 2020 Agnico Eagle Review
  - Borehole Collar / Borehole Trace

Fault traces are shown for an elevation of -400 masl.

CLIENT	 AGNICO EAGLE	
CONSULTANT	WSP	GOLDER
YYYY-MM-DD	2021-05-25	
PREPARED	HG	
DESIGNED	HG	
REVIEWED	JL	
APPROVED	DC	

PROJECT	AGNICO EAGLE MINES LIMITED MELIADINE EXTENSION NUNAVUT		
TITLE	BOREHOLE LOCATIONS FOR HYDRAULIC TESTING AND GROUNDWATER SAMPLING – MAIN AREA		
PROJECT NO.	22513890	PHASE	2000
REV.	0	FIGURE	4

25 mm IF THIS MEASUREMENT DOES NOT MATCH WHAT IS SHOWN, THE SHEET SIZE HAS BEEN MODIFIED FROM A3S-B

### 3.3.2 2015 Tiriganiaq Testing Program

To improve the level of confidence in the predictions of groundwater inflow quantity and quality for the Tiriganiaq Underground, a hydrogeology gap analysis was completed by WSP Golder in 2015 to 2016. Two independent technical advisors, Dr. Shaun K. Frape and Dr. Walter A. Illman (both from the University of Waterloo) provided advice and comments on the gap assessment.

The 2015 Underground Program (Golder 2016) was executed primarily within boreholes drilled from the Tiriganiaq underground development and consisted of the following hydraulic testing:

- 24 packer tests carried out over depth intervals ranging from 313 to 689 mbgs at three boreholes (TIS-200-001, TIS-200-002 and TIS-225-001)
- two flow recession pumping tests carried out from 327 to 593 mbgs and 592 to 689 mbgs below ground surface at TIS-200-002 and TIS-200-001 respectively, to characterize the storage properties and hydraulic conductivity of the bulk bedrock over a larger scale than can be tested by packer testing. During testing, one borehole acted as the pumping well and the other two boreholes as observation points
- two injection tests carried out at TIS-200-002 to investigate the option of reinjecting water back into the formation

A summary of the hydraulic test results is provided in Table 2, Table 3 and Table 4, with the location of the test holes presented on Figure 4. Results of the hydraulic tests indicate the following:

- Test 7 and 8 at TIS-200-001 intersected a potential fault, which is interpreted to be Fault A. The estimated transmissivity was between  $1 \times 10^{-6}$  m<sup>2</sup>/s to  $5 \times 10^{-7}$  m<sup>2</sup>/s over the tested intervals. Assuming a fault thickness of 5 m, this would indicate a hydraulic conductivity of between  $1 \times 10^{-7}$  m/s and  $2 \times 10^{-7}$  m/s. Analysis of the flow recession test in this borehole indicated a fault hydraulic conductivity of  $4 \times 10^{-8}$  m/s, which is slightly lower than that estimated from the single-well response test.
- Test 6 and 7 at TIS-225-001 intersected a potential fault (likely Fault A), however the transmissivity was low ( $2 \times 10^{-8}$  m<sup>2</sup>/s to  $5 \times 10^{-8}$  m<sup>2</sup>/s) and consistent with intervals with no identified fault. This may indicate the transmissivity of the faults is variable along its length, which is not unexpected.
- At TIS-200-002, Test 5 is interpreted to have intercepted RM175. The transmissivity was estimated at  $1 \times 10^{-7}$  m<sup>2</sup>/s. Assuming a fault thickness of 5 m, this would indicate a fault hydraulic conductivity of  $2 \times 10^{-8}$  m/s.
- Results of both pumping tests indicate that the specific storage in the bedrock of the Wesmeg Formation to be on the order of  $1 \times 10^{-7}$  1/m to  $2 \times 10^{-7}$  1/m. At the time of the 2014 FEIS no site-specific information on the storage of the bedrock was available; therefore, in the FEIS, the specific storage was assumed to be  $1 \times 10^{-6}$  1/m.

**Table 2: Summary of Packer Tests – 2015 Underground Program**

Borehole ID	Test Number	Interval Top (mbgs)	Interval Bottom (mbgs)	Interval Length (m vertical depth)	Interval Length (mah)	Structural Feature	Transmissivity (m <sup>2</sup> /s)	Hydraulic Conductivity <sup>1</sup> (m/s)	Rock Type
TIS-200-001	Test 1	318.3	364.3	46.0	49.7	--	$3 \times 10^{-08}$	$5 \times 10^{-10}$	Mafic
TIS-200-001	Test 2	368.0	407.1	39.1	41.4	--	$3 \times 10^{-09}$	$<1 \times 10^{-10}$	Mafic
TIS-200-001	Test 3	404.3	456.2	51.8	55.1	--	$1 \times 10^{-08}$	$2 \times 10^{-10}$	Mafic
TIS-200-001	Test 4	454.6	503.3	48.8	51.9	--	$7 \times 10^{-09}$	$1 \times 10^{-10}$	Mafic
TIS-200-001	Test 5	501.8	564.4	62.6	58.6	--	$1 \times 10^{-08}$ (a)	$1 \times 10^{-10}$ (a)	Mafic
TIS-200-001	Test 6	562.8	625.5	62.6	58.6	--	$1 \times 10^{-08}$ (a)	$1 \times 10^{-10}$ (a)	Mafic, Gabbro, Iron Formation, Ultramafic, Quartz Vein
TIS-200-001	Test 7	651.7	689.3	37.7	33.3	Joint, Fault A	$5 \times 10^{-07}$	$1 \times 10^{-08}$	Mafic, Gabbro, Iron Formation, Ultramafic
TIS-200-001	Test 8	623.9	689.3	65.4	57.9	Joint, Fault A	$1 \times 10^{-06}$	$1 \times 10^{-08}$	Mafic, Gabbro Iron formation, Ultramafic, Quartz ankerite Vein
TIS-225-001	Test 1	319.3	374.4	55.1	56.0	--	$3 \times 10^{-10}$	$<1 \times 10^{-10}$	Mafic
TIS-225-001	Test 2	422.2	440.2	18.0	17.7	--	$1 \times 10^{-08}$	$7 \times 10^{-10}$	Mafic
TIS-225-001	Test 3	377.8	440.2	62.5	54.9	--	$5 \times 10^{-09}$	$<1 \times 10^{-10}$	Mafic
TIS-225-001	Test 4	438.8	506.8	68.0	66.6	--	$3 \times 10^{-09}$	$<1 \times 10^{-10}$	Mafic
TIS-225-001	Test 5	505.4	567.9	62.5	61.2	--	$1 \times 10^{-08}$	$1 \times 10^{-10}$	Mafic, Iron formation
TIS-225-001	Test 6	608.1	629.0	20.8	18.4	Fault A	$5 \times 10^{-08}$	$2 \times 10^{-09}$	Ultramafic, Iron formation
TIS-225-001	Test 7	563.7	629.0	65.2	57.8	Fault A	$2 \times 10^{-08}$	$3 \times 10^{-10}$	Iron formation, Ultramafic
TIS-225-001	Test 8	627.6	692.8	65.2	57.8	Joint	$9 \times 10^{-08}$	$1 \times 10^{-09}$	Ultramafic, Mafic
TIS-200-002	Test 1	316.2	326.0	9.8	10.0	Joint	$3 \times 10^{-07}$	$3 \times 10^{-08}$ (b)	Mafic
TIS-200-002	Test 3	347.1	409.6	62.5	67.5	--	$2 \times 10^{-08}$	$3 \times 10^{-10}$	Mafic
TIS-200-002	Test 4	388.6	441.2	52.6	56.8	--	$2 \times 10^{-09}$	$<3 \times 10^{-10}$	Mafic
TIS-200-002	Test 5	444.1	506.9	62.8	67.8	RM175	$1 \times 10^{-07}$	$2 \times 10^{-09}$	Mafic
TIS-200-002	Test 6	505.1	548.5	43.4	46.8	--	$5 \times 10^{-08}$	$1 \times 10^{-09}$	Mafic
TIS-200-002	Test 7	378.6	425.5	43.4	49.8	--	$6 \times 10^{-08}$	$1 \times 10^{-09}$	Mafic
TIS-200-002	Test 10	327.2	592.9	265.7	287.2	--	$7 \times 10^{-10}$	$<1 \times 10^{-10}$	Mafic, Chert Iron formations
TIS-200-002	Test 11	592.3	689.3	97.1	104.9	Fault	$4 \times 10^{-8}$	$1 \times 10^{-10}$	Mafic, Chert Iron Formations

1) Calculated based on estimated transmissivity and test interval length; (a) Test could not be analyzed with analytical methods. Estimation only.

**Table 3: Summary of Flow Recession Pumping Tests – 2015 Underground Program**

Borehole ID	Interval Top (mbgs)	Interval Bottom (mbgs)	Interval Length (m vertical depth)	Interval Length (mah)	Hydraulic Conductivity (m/s)	Specific Storage (1/m)
TIS-200-002	327.2	592.9	265.7	286	$2 \times 10^{-10}$	$2 \times 10^{-7}$
TIS-200-001	592.3	689.3	97.1	104.9	$4 \times 10^{-8}$	$1 \times 10^{-7}$

**Table 4: Summary of Injection Trial Results in TIS-200-022 – 2015 Underground Program**

Test ID <sup>b</sup>	Cycle #	Average Pressure (Mpa) <sup>a</sup>	Average Flow Rate (L/min) <sup>a</sup>	Estimated Transmissivity (m <sup>2</sup> /s)	Estimated Hydraulic Conductivity (m/s)
Test 1	1	3.2	0.4	$8 \times 10^{-08}$	$2 \times 10^{-10}$
	2	4.3	0.8	$7 \times 10^{-08}$	$2 \times 10^{-10}$
	3	4.8	0.7	$6 \times 10^{-08}$	$2 \times 10^{-10}$
	4	5.4	0.9	$6 \times 10^{-08}$	$2 \times 10^{-10}$
	5	5.9	0.9	$5 \times 10^{-08}$	$1 \times 10^{-10}$
	6	6.5	1.8	$9 \times 10^{-08}$	$2 \times 10^{-10}$
	7	7.0	2.7	$1 \times 10^{-07}$	$3 \times 10^{-10}$
	8	7.4	4.6	$2 \times 10^{-07}$	$5 \times 10^{-10}$
	9	7.6	7.0	$3 \times 10^{-07}$	$7 \times 10^{-10}$
	10	8.3	11.5	$4 \times 10^{-07}$	$1 \times 10^{-9}$
Test 2	1	3.3	1.1	$2 \times 10^{-07}$	$4 \times 10^{-10}$
	2	3.9	1.4	$1 \times 10^{-07}$	$4 \times 10^{-10}$
	3	4.7	1.8	$1 \times 10^{-07}$	$4 \times 10^{-10}$
	4	5.0	1.9	$1 \times 10^{-07}$	$3 \times 10^{-10}$
	5	5.6	1.8	$1 \times 10^{-07}$	$3 \times 10^{-10}$
	6	6.4	2.5	$1 \times 10^{-07}$	$3 \times 10^{-10}$
	7	7.0	3.4	$1 \times 10^{-07}$	$4 \times 10^{-10}$
	8	7.8	5.2	$2 \times 10^{-07}$	$5 \times 10^{-10}$
	9	8.3	8.8	$3 \times 10^{-07}$	$8 \times 10^{-10}$
	10	8.5	13.9	$5 \times 10^{-07}$	$1 \times 10^{-9}$

a) Average from last five minutes of the test. b) Tests conducted between approximately 330 and 730 mbgs.

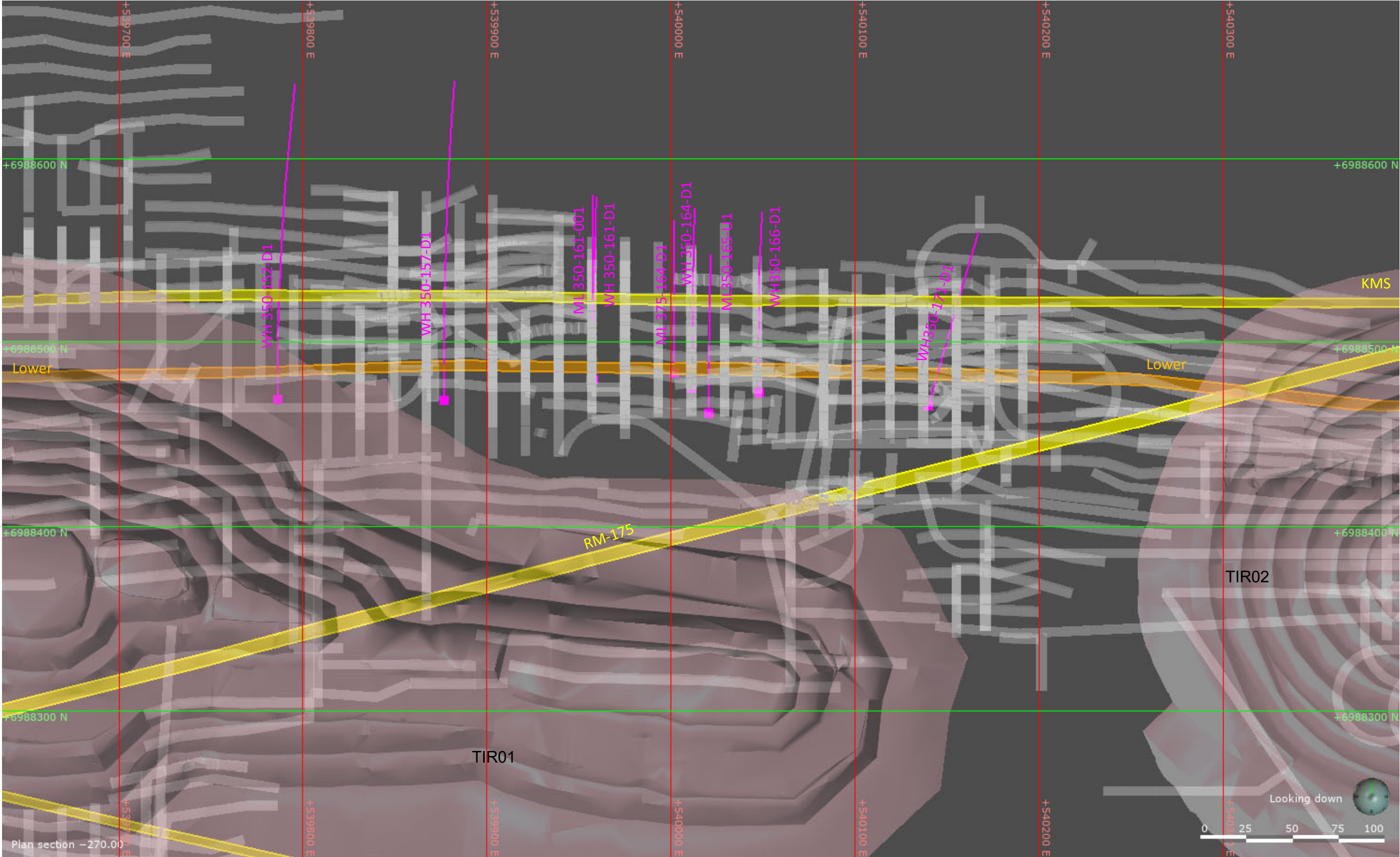
### 3.3.3 2019-2020 Tiriganiaq Testing Program

In 2019 and 2020, Hydro-Resources Inc. on behalf of Agnico Eagle conducted short-term (few hours) and long-term (several days) recession tests from the Tiriganiaq underground in a series of 14 boreholes targeting the KMS corridor near the interpreted KMS fault and Lower Fault Zone (Figure 5). Data collection from the short-term recession tests were generally limited and did not provide reliable estimation of hydraulic conductivity; however, the long-term recession test conducted over approximately 72 hrs at WH350-157-D1 in July 2020 provided a good data set for estimation of the corridor hydraulic conductivity.

Hydro-Resources Inc. estimated transmissivity based on distance draw down analysis. Tested boreholes were both partially penetrating in some cases and extending past the outer limits of the corridor in others. Assuming an average interpreted corridor thickness of approximately 100 m, the hydraulic conductivity of the corridor was estimated from the provided transmissivity values to range between  $2 \times 10^{-7}$  m<sup>2</sup>/s and  $1 \times 10^{-6}$  m<sup>2</sup>/s with a geometric average of  $4 \times 10^{-7}$  m<sup>2</sup>/s, indicating that the corridor is a zone of enhanced permeability.

Based on the collected pressure response data, a screening-level estimation of the hydraulic diffusivity was also calculated from the distance between the observation points and the pumped borehole, and the observed time for the first pressure response in the well. Hydraulic diffusivity gives a measure of diffusion speed of pressure disturbances in a groundwater system, and for consistent hydrostratigraphic units, the calculated diffusivity should be similar. Table 5 presents a summary of the calculated diffusivity, and indicates a wide range of hydraulic diffusivity, with values between  $<1$  m<sup>2</sup>/s and 791 m<sup>2</sup>/s. This variability indicates changes in the bedrock hydraulic properties between the pumped borehole and the observation points. For example, at PZ-ML375-194-D1-VW1 and VW3, the first response at the VW1 sensor was within 30 minutes whereas at VW3 it was after 85 m despite being relatively equal distance for the pumping well. This indicates that the KMS corridor may be composed of multiple discrete fractures with competent rock in between the fractures and that this compartmentalization results in heterogeneity in the hydraulic response. Given the complexity of the corridor, the hydraulic conductivity of the corridor will be evaluated further as part of numerical model calibration.





**LEGEND**

- Regional Fault
- Supplemental Faults Based on 2020 Agnico Eagle Review
- Borehole Collar / Borehole Trace

Fault traces are shown for an elevation of -270 masl.

CLIENT



CONSULTANT



YYYY-MM-DD 2021-05-25

PREPARED HG

DESIGNED HG

REVIEWED JL

APPROVED DC

PROJECT

AGNICO EAGLE MINES LIMITED  
MELIADINE EXTENSION  
NUNAVUT

TITLE

**BOREHOLE LOCATIONS FOR HYDRAULIC TESTING AND  
GROUNDWATER SAMPLING – KMS CORRIDOR**

PROJECT NO.  
22513890

PHASE  
2800

REV.  
0

FIGURE  
5

**Table 5: Summary of Estimated Hydraulic Conductivity and Diffusivity Values from Long Term Recession Test at WH350-157-D1**

K (m/s)	Test Location	Observation Point												
	WH350-157-D1	WH350-161-D1	WH350-164-D1	ML350-165-U1	WH350-166-D1	PZ-WH350-152-VW1	PZ-WH350-152-VW2	PZ-WH350-152-VW3	PZ-ML17-350-161-VW1	PZ-ML17-350-161-VW2	PZ-WH350-171-D1-VW1	PZ-WH350-171-D1-VW2	PZ-ML375-164-D1-VW1	PZ-ML375-164-D1-VW3
Approximate Depth (mbgs) <sup>b</sup>	337	334	337	335	334	331	335	340	323	323	341	343	361	374
Hydraulic Conductivity (m/s) <sup>(a)</sup>	-	$3 \times 10^{-7}$	$1 \times 10^{-6}$	$7 \times 10^{-7}$	$8 \times 10^{-7}$	$3 \times 10^{-7}$	$3 \times 10^{-7}$	$3 \times 10^{-7}$	$3 \times 10^{-7}$	$3 \times 10^{-7}$	$5 \times 10^{-7}$	$5 \times 10^{-7}$	$3 \times 10^{-7}$	$2 \times 10^{-7}$
Time to First Response (min)	NA	1	1	2	1	1	1	1	1	1	30	30	85	1
Distance to Pumping Well (m)	0	82	135	150	171	88	88	88	106	103	269	278	129	132
Calculated Diffusivity (m <sup>2</sup> /s)	NA	545.5	410.7	73	790.7	323.8	310.2	310.2	72.2	68.2	10.3	11	0.8	190.5

a) Assuming an interpreted corridor thickness of 100 m. b) Approximate depth represents mid point of open borehole or elevation of vibrating wire sensor (VW1/VW2/VW3). Depth assumes a ground surface elevation of approximately 55 m.



### 3.3.4 2020 Discovery Testing Program

In May and June 2020, hydraulic testing was conducted in two boreholes in the proposed Discovery underground area. Seven tests were conducted at M20-2984 (DISCO-CONV-016) using packers at depths of between 5 and 499 mbgs and 5 tests were conducted at M20-2989 (DISCO-CONV-021-V2) using packers at depths of between 254 and 611 mbgs. A zone of enhanced permeability was interpreted in borehole M20-2984 between 512 and 524 mah, which has been interpreted to correspond to Fault 2 based fault locations provided by Agnico Eagle (Section 3.2). Hydraulic conductivity values calculated for the test intervals #2, 3, 4 and 7 that straddle the interpreted structure range from  $6 \times 10^{-8}$  to  $4 \times 10^{-7}$  m/s indicating moderate to low hydraulic conductivity. Transmissivity values calculated for these intervals ( $3 \times 10^{-6}$  m<sup>2</sup>/s to  $6 \times 10^{-6}$  m<sup>2</sup>/s,) demonstrate that despite the difference in test interval lengths the pressure responses in these tests are largely controlled by the properties of the enhanced permeability zone. Assuming a uniform thickness of 12 m, the hydraulic conductivity of the enhanced permeability zone was estimated to be between  $3 \times 10^{-7}$  m/s and  $5 \times 10^{-7}$  m/s, indicating a moderate hydraulic conductivity. A summary of the hydrogeological test results is summarized on Table 5 and documented in Golder (2021a).

In August 2020, 13 single-well response tests were conducted at borehole M20-3071, located to the west of the proposed Discovery underground near Lake CH6 (Figure 3). The first 8 tests were packer tests completed between approximately 166.9 mbgs and 560.7 mbgs. The last five tests were conducted after the installation of a Westbay system in the borehole and were conducted at Ports 7, 8, 9, 10 and 11. The transmissivity and bulk hydraulic conductivity in these port intervals were estimated from the pressure response data collected by transducers within the sampling cylinders of the Westbay system. A summary of the hydrogeological test results is summarized on Table 6 and documented in Golder (2021d). Overall, hydraulic conductivity estimates ranged from less than  $1 \times 10^{-10}$  m/s to  $6 \times 10^{-9}$  m/s.

**Table 6: Summary of Hydraulic Test Results Near Discovery Underground – Fall of 2020**

Borehole	Test Number	Interval Top (mbgs)	Interval Bottom (mbgs)	Interval length (mbgs)	Interval Length (mah)	Transmissivity (m <sup>2</sup> /s)	Hydraulic Conductivity (m/s)	Geology
M20-2984	1 <sup>(b)</sup>	256.4	388.1	131.7	142.4	$6 \times 10^{-7(b)}$	$1 \times 10^{-9(b)}$	Greywacke and Siltstone, Chert-Magnetite Iron Formation
M20-2984	2 <sup>(b)</sup>	397.9	485.4	87.4	94.5	$6 \times 10^{-6}$	$7 \times 10^{-8}$	Greywacke and Siltstone, Chert-Magnetite Iron Formation, Fault 2
M20-2984	3 <sup>(b)</sup>	470.1	485.4	15.3	16.5	$6 \times 10^{-6}$	$4 \times 10^{-7}$	Greywacke and Siltstone, Chert-Magnetite Iron Formation, Fault 2
M20-2984	4 <sup>(b)</sup>	389.6	485.4	95.8	103.5	$6 \times 10^{-6}$	$5 \times 10^{-8}$	Greywacke and Siltstone, Chert-Magnetite Iron Formation, Fault 2
M20-2984	5 <sup>(b)</sup>	483.8	499.2	15.5	16.7	$8 \times 10^{-8}$	$5 \times 10^{-9}$	Gabbro, Greywacke and Siltstone, Chert-Magnetite Iron Formation
M20-2984	6 <sup>(c)</sup>	4.6	499.2	494.6	534.6	(c)	(c)	Greywacke and Siltstone, Chert-Magnetite Iron Formation,
M20-2984	7	464.3	499.2	35.0	37.8	$3 \times 10^{-6}$	$8 \times 10^{-8}$	Gabbro, Greywacke and Siltstone, Chert-Magnetite Iron Formation, Fault 2
M20-2989	1 <sup>(c)</sup>	254.5	535.7	281.2	303.9	(c)	(c)	Chloritic Siltstone and Greywacke, Altered Mafic Volcanics
M20-2989	2 <sup>(b)</sup>	254.5	566.2	311.7	336.9	$5 \times 10^{-6}$	$2 \times 10^{-8}$	Chloritic Siltstone and Greywacke, Altered Mafic Volcanics
M20-2989	3 <sup>(b)</sup>	376.6	566.2	189.6	204.9	$2 \times 10^{-6}$	$9 \times 10^{-9}$	Siltstone, Greywacke and Siltstone
M20-2989	4 <sup>(b)</sup>	326.6	566.2	239.6	258.9	$1 \times 10^{-6}$	$4 \times 10^{-9}$	Altered Mafic Volcanics, Siltstone, Greywacke and Siltstone
M20-2989	5	418.2	610.6	192.4	207.9	$7 \times 10^{-7}$	$3 \times 10^{-9}$	Greywacke and Siltstone
M20-3071	1	171.9	213.8	41.9	44.6	$5 \times 10^{-8}$	$1 \times 10^{-9}$	Chloritic Siltstone and Greywacke
M20-3071	2	211.1	250.3	39.2	41.9	$3 \times 10^{-9}$	$<1 \times 10^{-10}$	Chloritic Siltstone and Greywacke
M20-3071	3	246.5	286.4	39.9	42.0	$3 \times 10^{-7}$	$6 \times 10^{-9}$	Chloritic Siltstone and Greywacke
M20-3071	4	283.7	325.1	41.4	45.0	(c)	(c)	Chloritic Siltstone and Greywacke
M20-3071	5	325.5	360.9	35.4	38.6	$<2 \times 10^{-10}$	$<1 \times 10^{-10}$	Chloritic Siltstone and Greywacke
M20-3071	6	404.7	447.9	43.2	47.8	$6 \times 10^{-10}$	$<1 \times 10^{-10}$	Chloritic Siltstone and Greywacke

**Table 6: Summary of Hydraulic Test Results Near Discovery Underground – Fall of 2020**

Borehole	Test Number	Interval Top (mbgs)	Interval Bottom (mbgs)	Interval length (mbgs)	Interval Length (mah)	Transmissivity (m <sup>2</sup> /s)	Hydraulic Conductivity (m/s)	Geology
M20-3071	7	358.1	447.9	89.8	99.0	$1 \times 10^{-9}$	$<1 \times 10^{-10}$	Chloritic Siltstone and Greywacke
M20-3071	8	445.2	561.0	115.8	129.0	$7 \times 10^{-9}$	$<1 \times 10^{-10}$	Chloritic Siltstone and Greywacke, Chert-Magnetite Iron Formation
M20-3071	Port 11	243	273.3	30.3	32.6	$2 \times 10^{-8}$	$5 \times 10^{-10}$	Chloritic Siltstone and Greywacke
M20-3071	Port 10	274.1	291.7	17.6	19.0	$7 \times 10^{-8}$	$4 \times 10^{-9}$	Chloritic Siltstone and Greywacke
M20-3071	Port 9	292.5	310.0	17.5	18.9	$7 \times 10^{-9}$	$4 \times 10^{-10}$	Chloritic Siltstone and Greywacke
M20-3071	Port 8	310.8	326.9	16.1	17.5	$6 \times 10^{-8(a)}$	$3 \times 10^{-9(a)}$	Chloritic Siltstone and Greywacke
M20-3071	Port 7	327.7	382.5	54.8	60.0	$1 \times 10^{-9(a)}$	$<1 \times 10^{-10(a)}$	Chloritic Siltstone and Greywacke

a) Low to moderate confidence in the result due to small magnitude of pressure change during the test.

b) Results are estimate only because the static conditions were not reached prior to test.

c) Results not reliable due to packer bypass observed during test.

d) Low to moderate confidence in the result due to small magnitude of pressure change during the test.

mbgs = metres below ground surface, mah = metres along hole.

### 3.3.5 2021 Geotechnical Site Investigation

In 2021, Tetra Tech Canada Inc. on behalf of Agnico Eagle conducted five packer tests in shallow boreholes drilled near the A6 Berm, CP9 Dike, D-B7 West Drainage Boundary and B5 North Berm (Tetra Tech 2021). Of these tests, testing at GT21-73 was considered by Tetra Tech to have poor data quality; data at GT21-20 and GT21-102 to have moderate data quality; and data at GT21-60 and GT21-100 to have good data quality. Hydraulic conductivity values of the shallow bedrock ranged from  $2 \times 10^{-7}$  m/s to  $1 \times 10^{-5}$  m/s (Table 7).

### 3.3.6 2021 Wesmeg Testing Program

In December 2020, three single-well response tests were conducted at borehole ML400-10197-D2 from Tiriganiaq underground towards the proposed Wesmeg underground (Golder 2021e). Test 1 and Test 3 were conducted in the competent bedrock and had estimated hydraulic conductivity values of  $4 \times 10^{-9}$  m/s and  $7 \times 10^{-10}$  m/s at depths between approximately 490 and 700 mbgs (Table 8). Two potential conductive zones were intercepted by the borehole with the Test 2 interval. These included an open joint between 257.9 and 258 mah, coinciding with the projected interception of Fault A, and a zone of poor core recovery (with evidence of fault gouge) intercepted at a depth of 300.9 mah and 301.4 mah. Fault A has an assumed thickness of 6 m based on Agnico Eagle's structural geology review. Assuming the hydraulic conductivity of Test 2 is controlled by Fault A with a general thickness of 6 m, the estimated hydraulic conductivity of the fault would be  $7 \times 10^{-8}$  m/s.

### 3.3.7 2021 Discovery Testing

In May and June 2020, hydraulic testing was conducted in borehole G21-98 near the proposed Discovery underground area (Golder 2022b) between depths of approximately 197 and 265 mbgs. Four of five tests were conducted in the competent bedrock with estimated hydraulic conductivity values ranging from  $8 \times 10^{-9}$  m/s to  $8 \times 10^{-8}$  m/s (Table 9). A zone of enhanced permeability was encountered within the Test 3 interval between 289.85 and 318.3 metres along hole. This zone coincides with lower rock quality designation (RQD) values between 315 and 321 metres along hole interpreted as Fault 1 by Agnico Eagle geologists. Fault 1 has an assumed thickness of 6 m based on Agnico Eagle's structural geology review, though the observed thickness of poor. Assuming a fault thickness of 6 m, the hydraulic conductivity of Fault 1 is estimated to be  $8 \times 10^{-7}$  m/s.

**Table 7: Summary of Hydraulic Tests Results from the 2021 Geotechnical Site Investigation**

General Area	Borehole	Test Number	Interval Top (mbgs)	Interval Bottom (mbgs)	Interval Length (m)	Hydraulic Conductivity (m/s)	Geology
A6 Berm	GT21-60 (35)	1	12.0	15.0	3.0	$5 \times 10^{-6}$	Greywacke
Dike D-CP9	GT21-20	2	11.0	15.5	4.5	$2 \times 10^{-7}$	Greywacke
B5 North Berm	GT21-100	3	9.0	12.0	3.0	$1 \times 10^{-5}$	Greywacke
D-B7 West	GT21-73	4	13.5	16.5	3.0	$2 \times 10^{-6}$ *	Greywacke
B5 North Berm	GT21-102	5	12.0	15.0	3.0	$3 \times 10^{-7}$	Greywacke

mbgs = metres below ground surface, mah = metres along hole, \* - testing interpreted to be poor data quality.

**Table 8: Summary of Hydraulic Tests Results from the 2021 Wesmeg Underground Testing Program**

Borehole	Test Number	Interval Top (mbgs)	Interval Bottom (mbgs)	Interval length (m vertical)	Interval Length (mah)	Transmissivity ( $m^2/s$ )	Hydraulic Conductivity (m/s)	Geology
ML400-10197-D2	1	493.0	584.8	91.9	100.6	$4 \times 10^{-7}$	$4 \times 10^{-9}$	Mafic Volcaniclastics
ML400-10197-D2	2	583.3	650.6	67.3	73.7	$4 \times 10^{-7}$	$5 \times 10^{-9}$	Mafic Volcaniclastics, Fault A
ML400-10197-D2	3	659.0	699.9	40.9	44.8	$3 \times 10^{-8}$	$7 \times 10^{-10}$	Mafic Volcaniclastics

mbgs = metres below ground surface, mah = metres along hole.

**Table 9: Summary of Hydraulic Tests Results Near Discovery Underground – Fall 2021**

Borehole	Test Number	Interval Top (mbgs)	Interval Bottom (mbgs)	Interval length (m vertical depth)	Interval Length (mah)	Transmissivity (m <sup>2</sup> /s)	Hydraulic Conductivity (m/s)	Geology
GT21-98	1	197.2	208.0	10.7	13.7	$1 \times 10^{-7}$	$8 \times 10^{-9}$	Greywacke and Siltstone
GT21-98	2	206.8	226.8	20.0	25.5	$9 \times 10^{-7}$	$4 \times 10^{-8}$	Greywacke and Siltstone, Chert-Chlorite Iron Formation
GT21-98	3	228.1	250.4	22.4	28.5	$5 \times 10^{-6}$	$2 \times 10^{-7}$	Chert-Chlorite Iron Formation, Chlorite Siltstone and Greywacke, Fault #1
GT21-98	4	253.7	264.6	10.9	13.9	$1 \times 10^{-6}$	$8 \times 10^{-8}$	Chlorite Siltstone and Greywacke
GT21-98	5	246.6	264.6	18.0	22.9	$4 \times 10^{-7}$	$2 \times 10^{-8}$	Chlorite Siltstone and Greywacke

mbgs = metres below ground surface, mah = metres along hole.

### 3.3.8 2021 Pump, Wesmeg, Fzone, and Lake B5 Testing Programs

In February and September 2021, hydraulic testing was near Lake B5 and the proposed Pump, Wesmeg, F Zone undergrounds (Golder 2022a). Table 10 presents a summary of the estimated hydraulic conductivity values for the testing, with additional detail below.

- **Pump Underground (M21-3255)** – Eighteen packer tests were completed at M21-3255 to estimate the hydraulic conductivity of the bedrock near Pump underground between depths of 20 and 500 mbgs. Twelve tests were completed in competent bedrock and had estimated hydraulic conductivity values of between  $2 \times 10^{-10}$  m/s and  $2 \times 10^{-5}$  m/s (Table 10). The highest hydraulic conductivity values were generally associated with the more altered shallow bedrock in the upper 75 m of depth. Five of the tests intersected a low RQD zone, and had estimated hydraulic conductivity values between  $2 \times 10^{-8}$  to  $1 \times 10^{-6}$  m/s. One test (Test 19) was completed across the Pyke Fault. Pyke Fault has an assumed thickness of 15 m based on Agnico Eagle's structural geology review. Assuming a fault thickness of 15m, and that the fault controlled the transmissivity in the test interval, the hydraulic conductivity of Pyke Fault was estimated to  $7 \times 10^{-10}$  m/s at that location.
- **Wesmeg Underground (M21-3250)** – Nine successful packer tests were completed at M21-3250, located near the proposed Wesmeg Underground, between depths of 126 and 454 mbgs. Five of the nine tests were completed in competent bedrock and had estimated hydraulic conductivity values of between  $4 \times 10^{-10}$  m/s and  $2 \times 10^{-7}$  m/s (Table 10). Test 3 was conducted across Fault C. Assuming a fault thickness of 3 m based on information from Agnico Eagle geologists, this would correspond to an estimated hydraulic conductivity of  $4 \times 10^{-9}$  m/s. Tests 8, 9 and 11 were conducted across PU\_NW\_1 / PU\_NW\_2. Assuming a fault thickness of 3 m based on information from Agnico Eagle geologists, this would correspond to an estimated hydraulic conductivity of between  $2 \times 10^{-10}$  to  $2 \times 10^{-9}$  m/s.
- **Fzone Underground (M21-3244)** – Eight packer tests were completed at M21-3244 to estimate the hydraulic conductivity of the bedrock near F Zone underground between depths of 107 and 402 mbgs. Five of the eight tests were completed in competent bedrock and had an estimated hydraulic conductivity values of between  $2 \times 10^{-9}$  m/s and  $5 \times 10^{-8}$  m/s (Table 10). Two tests (6 and 7) cross the Pike Fault, which has an assumed thickness of 15 m based on Agnico Eagle's structural geology review. Assuming a fault thickness of 15m, and that the fault controlled the transmissivity in the test interval, the hydraulic conductivity of Pyke Fault was estimated to be  $7 \times 10^{-9}$  to  $3 \times 10^{-7}$  m/s at those locations. An unknown fault was potentially intersected in Test interval 2. The transmissivity was low ( $7 \times 10^{-8}$  m/s) and assuming a thickness of 5 m, the fault would have an estimated hydraulic conductivity of  $1 \times 10^{-8}$  m/s. This hydraulic conductivity is like other competent bedrock tests at that depth.

- **Lake B5 (M21-3277)** – Ten successful packer tests were conducted at M21-3277 below Lake B5. Six of the ten tests were in competent bedrock, with estimated hydraulic conductivity values of between less than  $1 \times 10^{-10}$  m/s and  $5 \times 10^{-8}$  m/s (Table 10). Test 1 intersected the KMS Fault and Lower Fault zone. Assuming the KMS and Lower Fault zone straddled the entire interval, the hydraulic conductivity of fault was estimated at  $1 \times 10^{-8}$  m/s. Assuming an intercepted fault thickness of 5 m (Lower Fault Zone), the hydraulic conductivity of the faults is estimated to be  $1 \times 10^{-7}$  m/s. Test 11 is interpreted to have intersected ENE Fault 1, Fault A, and an open joint. Assuming the faults straddled the entire interval, the hydraulic conductivity of fault was estimated at  $7 \times 10^{-9}$  m/s. Assuming each structure had an approximate thickness of 5 m, the faults have an estimated hydraulic conductivity of  $3 \times 10^{-8}$  m/s. Test 12 encountered an unnamed fault, though the testing interval overlaps with the Test 11 interval, which is interpreted to have intersected the ENE Fault 1, Wesmeg A and an open joint. Assuming an approximate fault thickness of 5 m, the fault has an estimated hydraulic conductivity of  $2 \times 10^{-8}$  m/s.



**Table 10: Summary of Hydraulic Tests Results in 2020-2021 Underground Program**

Borehole	Test Number	Interval Top (mbgs)	Interval Bottom (mbgs)	Interval length (m vertical depth)	Interval Length (mah)	Transmissivity (m <sup>2</sup> /s)	Hydraulic Conductivity (m/s)	Geology
M21-3250	1	126.2	141.3	15.1	16.7	$8 \times 10^{-9}$	$5 \times 10^{-10}$	Mafic
M21-3250	2	145.1	179.3	34.1	37.7	$3 \times 10^{-8}$	$8 \times 10^{-10}$	Mafic
M21-3250	3	177.7	193.0	15.3	16.9	$7 \times 10^{-9}$	$4 \times 10^{-10}$	Mafic , Fault C
M21-3250	5	224.0	269.2	45.2	49.9	$3 \times 10^{-7}$	$6 \times 10^{-9}$	Mafic
M21-3250	6	270.2	307.2	37.0	40.9	$3 \times 10^{-7}$	$8 \times 10^{-9}$	Mafic
M21-3250	8	305.6	339.9	34.2	37.8	$5 \times 10^{-7}$	$1 \times 10^{-8}$	Mafic , NW1
M21-3250	9	338.2	377.9	39.8	43.9	$1 \times 10^{-7}$	$2 \times 10^{-9}$	Mafic , NW1
M21-3250	10	376.2	416.0	39.8	43.9	$1 \times 10^{-5}$	$2 \times 10^{-7}$	Mafic
M21-3250	11	414.3	454.1	39.8	43.9	$6 \times 10^{-8}$	$1 \times 10^{-9}$	Mafic , Fault
M21-3255	1	20.3	42.8	22.5	25.2	$4 \times 10^{-4}$	$2 \times 10^{-5}$	Mafic
M21-3255	2	41.7	66.8	25.1	28.2	$2 \times 10^{-4}$	$6 \times 10^{-6}$	Mafic
M21-3255	3	65.8	77.5	11.8	13.2	$2 \times 10^{-5}$	$1 \times 10^{-6}$	Mafic , Low RQD
M21-3255	5	111.2	131.0	19.8	22.2	$2 \times 10^{-6}$	$7 \times 10^{-8}$	Mafic , Low RQD
M21-3255	6	128.6	160.4	31.8	35.7	$6 \times 10^{-6}$	$2 \times 10^{-7}$	Mafic , Low RQD
M21-3255	7	159.3	171.1	11.8	13.2	$3 \times 10^{-6}$	$2 \times 10^{-7}$	Mafic
M21-3255	8	170.0	211.2	41.2	46.2	$1 \times 10^{-6}$	$2 \times 10^{-8}$	Mafic
M21-3255	9	209.7	238.4	28.7	32.2	$2 \times 10^{-6}$	$5 \times 10^{-8}$	Mafic
M21-3255	10	236.3	275.8	39.4	44.3	$2 \times 10^{-6}$	$6 \times 10^{-8}$	Mafic
M21-3255	11	92.2	110.4	18.2	20.5	$2 \times 10^{-6}$	$9 \times 10^{-8}$	Mafic , Low RQD
M21-3255	12	77.0	95.3	18.2	20.5	$3 \times 10^{-6}$	$2 \times 10^{-8}$	Mafic , Low RQD
M21-3255	13	274.0	315.9	41.9	47.0	$1 \times 10^{-7}$	$3 \times 10^{-10}$	Mafic
M21-3255	14	314.0	353.3	39.3	44.1	$1 \times 10^{-8}$	$3 \times 10^{-10}$	Mafic
M21-3255	15	351.4	382.7	31.3	35.1	$5 \times 10^{-7}$	$1 \times 10^{-8}$	Mafic
M21-3255	16	380.8	401.6	20.8	23.4	$4 \times 10^{-9}$	$2 \times 10^{-10}$	Mafic

**Table 10: Summary of Hydraulic Tests Results in 2020-2021 Underground Program**

Borehole	Test Number	Interval Top (mbgs)	Interval Bottom (mbgs)	Interval length (m vertical depth)	Interval Length (mah)	Transmissivity (m <sup>2</sup> /s)	Hydraulic Conductivity (m/s)	Geology
M21-3255	17	399.5	438.8	39.4	44.2	$6 \times 10^{-8}$	$1 \times 10^{-9}$	Mafic
M21-3255	18	436.9	465.6	28.6	32.2	$5 \times 10^{-8}$	$2 \times 10^{-9}$	Mafic
M21-3255	19	463.6	499.9	36.2	40.7	$1 \times 10^{-8}$	$3 \times 10^{-10}$	Mafic , Pyke Fault
M21-3244	1	107.2	144.1	36.9	40.7	$9 \times 10^{-8}$	$2 \times 10^{-9}$	Mafic
M21-3244	2	142.6	171.3	28.7	31.7	$7 \times 10^{-8}$	$2 \times 10^{-9}$	Mafic , Fault
M21-3244	3	169.8	209.4	39.6	43.7	$2 \times 10^{-7}$	$5 \times 10^{-9}$	Mafic
M21-3244	4	208.0	247.4	39.5	43.5	$5 \times 10^{-7}$	$1 \times 10^{-8}$	Mafic
M21-3244	5	245.8	285.5	39.7	43.8	$1 \times 10^{-7}$	$2 \times 10^{-9}$	Mafic
M21-3244	6	284.1	329.0	44.9	49.6	$5 \times 10^{-6}$	$1 \times 10^{-7}$	Mafic , Pyke Fault
M21-3244	7	327.6	337.1	9.6	10.5	$1 \times 10^{-7}$	$1 \times 10^{-8}$	Mafic , Pyke Fault
M21-3244	8	335.7	402.4	66.7	73.6	$4 \times 10^{-6}$	$5 \times 10^{-8}$	Mafic
M21-3277	1	153.2	201.9	48.7	49.7	$5 \times 10^{-7}$	$1 \times 10^{-8}$	Mafic , KMS Fault, Lower Fault
M21-3277	2	229.6	240.1	10.5	10.7	$5 \times 10^{-7}$	$5 \times 10^{-8}$	Mafic
M21-3277	3	256.1	290.1	34.0	34.7	$2 \times 10^{-7}$	$5 \times 10^{-9}$	Mafic
M21-3277	4	317.8	357.7	39.9	40.7	$3 \times 10^{-7}$	$7 \times 10^{-9}$	Mafic
M21-3277	8	113.9	173.3	59.4	60.6	$1 \times 10^{-9}$	$<1 \times 10^{-10}$ (a)	Mafic
M21-3277	9	84.5	143.8	59.3	60.5	$1 \times 10^{-9}$	$<1 \times 10^{-10}$ (a)	Mafic
M21-3277	10	352.1	396.9	44.8	45.7	$8 \times 10^{-7}$	$2 \times 10^{-8}$	Mafic
M21-3277	11	393.3	444.0	50.7	51.7	$4 \times 10^{-7}$	$7 \times 10^{-9}$	Mafic , ENE Fault 1, Wesmeg A, Open Joint
M21-3277	12	439.9	458.7	18.7	19.1	$9 \times 10^{-8}$	$4 \times 10^{-9}$	Mafic, Fault
M21-3277	13	457.6	491.0	33.4	34.1	$8 \times 10^{-7}$	$2 \times 10^{-8}$	Mafic

a) Low to moderate confidence in the result due to small magnitude of pressure change during the test..

b) Results not reliable due to packer bypass observed during test.

mbgs = metres below ground surface, mah = metres along hole.

## 3.4 Groundwater Sampling

### 3.4.1 Data Collection

In support of the 2014 FEIS, groundwater sampling was conducted to characterize the groundwater quality, in particular the salinity as indicated by total dissolved solids (TDS), as presented on Figure 6. This testing included:

- one sample in borehole GT09-19 from 105 mbgs collected in 2009 (Golder 2009). This well is located within the talik of Lake B7
- samples from eight intervals of the Westbay Monitoring Well M11-1157 (located near Tiriganiaq) at depths from 450 to 620 mbgs, below the base of the permafrost. Groundwater samples were collected from this well over four seasons, from 2011 to 2014 (Agnico Eagle 2014a; Agnico Eagle 2014b), with the 2014 sample being collected following the FEIS

Supplemental data has been collected since the FEIS near the Tiriganiaq underground between 2015 and 2022 and used to provide information on the lateral variability of groundwater quality (TDS) across the Tiriganiaq underground. This data is included on Figure 5 and consists of:

- three groundwater samples collected by Agnico Eagle from seeps near the top of the cryopeg that were identified within the Tiriganiaq underground development completed to November 2015
- eight groundwater samples collected by Golder (2016) from borehole TIS-200-001 near the Tiriganiaq underground during a 96-hour pumping test carried from 630 to 725 m depth below ground, directly below the underground development
- Fourteen (14) groundwater samples and 11 groundwater samples were collected by Agnico Eagle between 2021 and 2022 near the depths of 200 m and 300m below ground
- Opportunistic groundwater samples collected by Agnico Eagle / Hydro-Resources Inc from diamond drill holes underground between 2016 and 2021 (located between approximately 230 and 470 m depth below ground)

In support of the Meliadine Extension, a second Westbay well (M20-3071) was also installed near the proposed Discovery Underground and potential talik below CH6 (Golder 2021c) (Figure 5). Two ports were selected for development and sampling (Port 8 at approximately 310 to 326 mbgs and Port 4 at approximately 439 to 457 mbgs), with 2021 and 2022 sampling and development results presented in two reports (Golder 2021b; Golder 2023). Port 8 sampling was selected to support assessment of water salinity in the talik between lake CH6 and the deeper regional groundwater flow of high salinity (below the regional permafrost). Port 4 sampling was selected to support assessment of water quality to be intercepted at the Discovery underground (i.e., it is at a similar elevation) the overall interpretation of regional water quality below the permafrost at similar depths. At the time of this report, only Port 8 results are considered appropriate for estimating formation groundwater quality (Golder 2021b; 2022c).

### 3.4.2 Groundwater Salinity Profile

In the Canadian Shield, concentrations of TDS in groundwater increase with depth, primarily in response to upward diffusion of deep-seated brines. The chemicals that contribute to TDS in shield brines are typically chloride and calcium, with sodium to a lesser degree, except in areas close to the ocean or areas that were submerged by oceans in the past (Séguin 1995) where sodium can be a significant contributor to TDS in groundwater. The major contributors to TDS in sea water are chloride and sodium. The salinity of deep groundwater samples collected to date from Meliadine are at the high end of what has been observed at other sites in the Canadian Shield at corresponding depths (Frape and Fritz 1987; Stotler et al. 2012; Dominion 2014). The relatively high proportion of sodium relative to calcium in the groundwater sample likely indicates the presence of relict sea water in bedrock. It is known that this area was largely overlain by seawater during the last period of glaciation (Dyke et al. 2003).

Figure 6 presents the TDS profile with depth from sites in the Canadian Shield and that of the Meliadine groundwater samples. The Frape and Fritz dataset (1987) presented on Figure 6 was developed based on chemical analyses of deep saline water collected by various investigators from several sites in the Canadian Shield. The Diavik dataset is based on site-specific data from Diavik, supplemented by information from the Lupin Mine site located about 200 km north of Diavik (Blowes and Logsdon 1997). The Meadowbank dataset (Golder 2004) was developed based on site specific data from the Meadowbank Mine site supplemented by the data sources discussed above (Frape and Fritz 1987; Blowes and Logsdon 1997). Of note is that the Meadowbank and Diavik datasets reflect talik groundwater rather than sub permafrost groundwater. The hydraulic connection with an overlying freshwater lake at these sites results in lower salinity at equivalent depths than has been observed below fully developed permafrost at the Project.

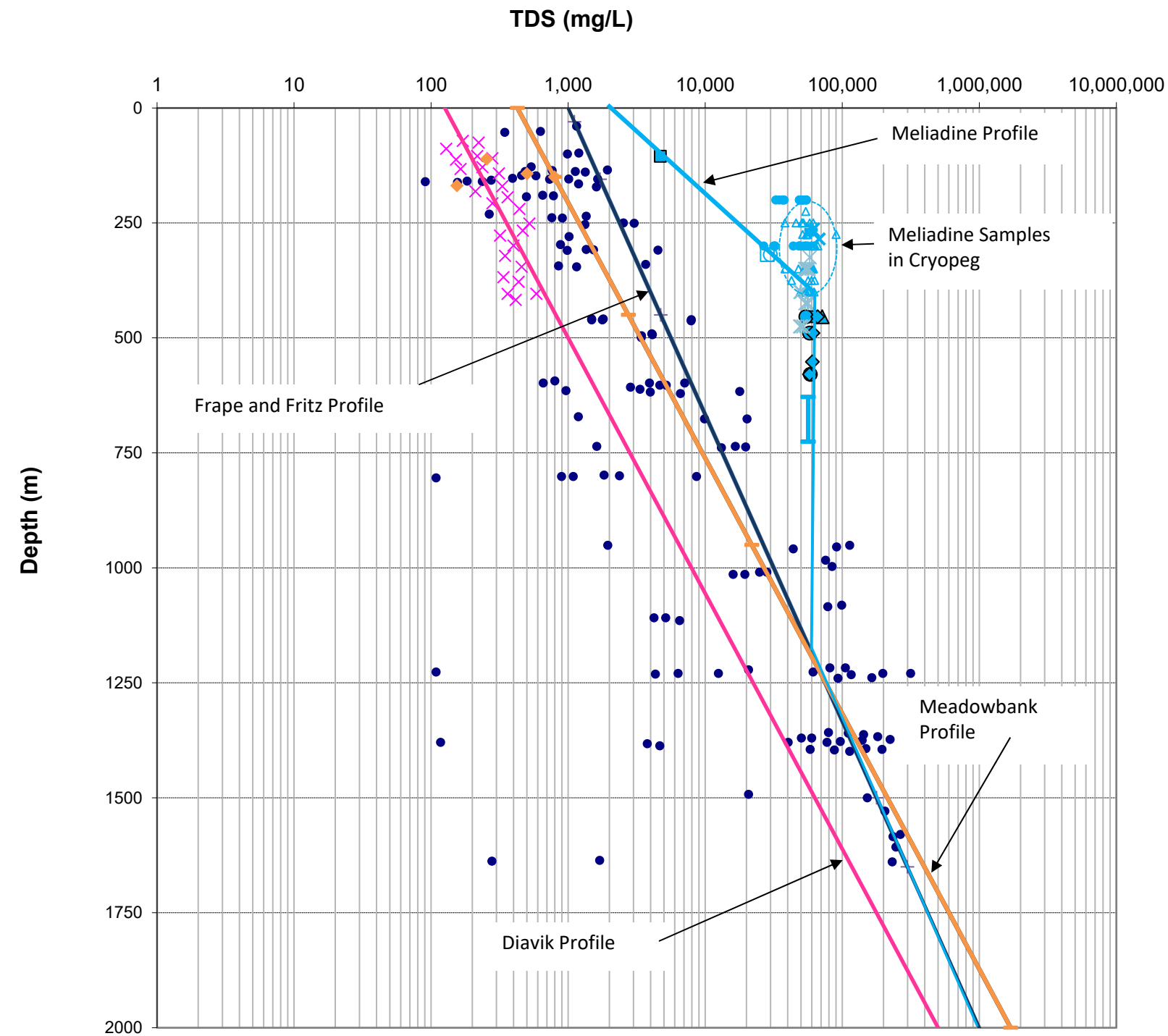
Although additional data has been collected to refine the profile, the interpreted TDS concentrations with depth is generally consistent with the TDS profile adopted in the FEIS (Agnico Eagle 2014a). Water quality in deep groundwater samplings suggest the salinity remains consistent with depth following the transition from near surface freshwater. Salinity concentrations in deep groundwater at Meliadine are approximately 1.5 times that of sea water (35 g/L).

Data collected from the underground diamond drill holes at Tiriganiaq are collected from depths between 230 and 475 m depth below ground. The circled tests on Figure 6 are inferred to be located above the zero-degree isotherm (base of permafrost) based on thermal modelling, and therefore within the cryopeg. TDS within the cryopeg may be elevated relative to groundwater in unfrozen rock at similar elevations due the preferential freezing of 'fresher' water and is similar to the assumed TDS below the regional permafrost (approximately 55,000 mg/L).

## 3.5 Permafrost Conditions

### 3.5.1 Depth to Permafrost and Lakes with Open Talik

Permafrost conditions at the time of the 2014 FEIS are described in SD 6-1 Permafrost Baseline Report in the 2014 FEIS (Agnico Eagle 2014a). Based on data at the time of the FEIS, the depth of permafrost was estimated to be on the order of 360 to 495 mbgs. Permafrost is defined as the zone extending from the bottom of the seasonally thawed layer (active layer) down to the 0-degree Celsius isotherm. The depth of the active layer ranges from approximately 1 to 3 m (Golder 2014).



- Multiple Sites (Frape and Fritz 1987)
- × Diavik (Kuchling et al. 2000)
- ◆ Meadowbank Data (Cumberland 2005)
- Meliadine GT09-19 - 2009 and M11-1257 - 2011 Samples
- ▲ Meliadine M11-1257 - 2012 Sample
- Meliadine M11-1257 - 2013 Sample
- ◆ Meliadine M11-1257 - 2014 Sample
- Meliadine 2015 - Underground Program
- × Meliadine 2015 Ramp Sample 1
- + Meliadine 2015 Ramp Sample 2
- × Meliadine 2015 Ramp Sample 3
- △ Meliadine 2016 and 2017 - DDH Holes Tiriganiaq
- Meliadine M20-3071 - 2020 Sample
- Meliadine M20-3071 - 2021 Sample
- ▲ Meliadine 2020 - DDH Holes Tiriganiaq
- × Meliadine 2021 - DDH Holes Tiriganiaq
- Meliadine 2021 Level 200 and 300 Sample

CLIENT



CONSULTANT



YYYY-MM-DD 2021-05-25

PREPARED HG

DESIGNED HG

REVIEWED JL

APPROVED DC

PROJECT

AGNICO EAGLE MINES LIMITED  
MELIADINE EXTENSION  
NUNAVUT

TITLE

**GROUNDWATER SALINITY PROFILE WITH DEPTH**

PROJECT NO.  
22513890

PHASE  
2000

REV.  
0

FIGURE  
6

When the size of a lake is above a critical value, the talik beneath the lake will be an open talik, which connects to the deep groundwater flow regime beneath the permafrost (Golder 2014). Beneath smaller lakes, which do not freeze to the bottom over the winter, a talik bulb that is not connected to the deep groundwater flow system will form (closed talik). Analytical solutions were used by Golder (2014) in support of the 2014 FEIS to evaluate the critical lake sizes to support open talik in consideration of geothermal gradient, mean annual ground temperature, mean annual lake bottom temperature and bathymetry. The analysis indicated that taliks extending through the permafrost will exist beneath circular lakes having a minimum radius of approximately 290 to 330 m and beneath elongate lakes having a minimum half width of approximately 160 to 195 m, without considering lake terrace geometries. When terrace effects are included in the analysis, the critical radius for a circular lake increases to between approximately 305 to 485 m, and the critical half width for an elongate lake increase to between approximately 170 and 280 m. These were based on assumptions that the terrace is 25% to 75% of the total lake width or diameter, respectively. In consideration of the analysis, it was inferred in the 2014 FEIS that near the Tiriganiaq deposit (the location of the proposed single underground at the time), Meliadine lake, Lake B7, Lake B8 and Lake D7 will have open taliks connected to the deep groundwater flow regime. Lake A8 and Lake B5 are considered possible from the analytical assessment, but less certain.

In support of the Meliadine Extension, two-dimensional (2D) thermal modelling was completed in 2020 (Golder 2021a) to evaluate regional permafrost conditions, assess the extent of lake taliks and to determine whether the proposed open pits and additional underground developments will remain within the permafrost limits. Thermal modelling was adopted over the analytical approach in the FEIS given the number of proposed undergrounds and proximity of these undergrounds to lakes with potential open taliks. The thermal model was recently updated in 2022 (Golder 2022) to include new data from deep thermistor strings installed within the Project area in 2021. The updated 2D thermal modelling considered data from 16 active thermistors in the Project area and one historical thermistor installed in the Tiriganiaq area (MW98-195). The location of thermistors installed at depths greater than 40 m within the Project area is shown in Appendix A and summarized in Table 11.

**Table 11: Thermistor Summary**

Location	Thermistor	Collar Coordinates					Depth Below Ground Surface (m)
		Northing (m)	Easting (m)	Elevation	Inclination (°)	Azimuth (°)	
Tiriganiaq	M98-195*	6,988,660	539,968	69	80	180	437
	GT09-19	6,989,458	537,899	63	51	325	152
	GT07-11	6,989,910	538,507	69	90	0	44
	GT07-10	6,988,805	538,506	69	90	0	44
	M21-3255 <sup>(a)</sup>	6,987,062	540,307	62	64	199	478
	M21-3250 <sup>(a)</sup>	6,987,915	539,750	64	67	181	370
	M21-3277 <sup>(a)</sup>	6,988,590	538,259	58	64	231	376
	M21-3276 <sup>(a)</sup>	6,988,948	539,779	70	79	188	493
F-Zone	GT09-07	6,986,260	542,429	60	60	204	130
	GT09-08	6,986,317	542,494	60	71	207	139
	M21-3244 <sup>(a)</sup>	6,986,412	542,045	62	67	156	402

**Table 11: Thermistor Summary**

Location	Thermistor	Collar Coordinates					Depth Below Ground Surface (m)
		Northing (m)	Easting (m)	Elevation	Inclination (°)	Azimuth (°)	
Discovery	DS09GT-03	6,981,625	554,379	72	67	54	129
	DS09GT-04	6,981,611	554,453	74	71	45	128
	DC-16	6,981,980	554,770	67	70	179	475
	DC-19	6,982,025	554,220	67	66	179	260
	DC-21	6,981,071	554,846	70	60	140	572

\* Historical thermistor.

a) M21-3255, M21-3250, M21-3277, M21-3276, and M21-3244 are reported as GT21-44, GT21-46, GT21-71, GT21-75, and GT21-59 in Golder (2022)

Two-dimensional thermal models were prepared for 21 cross-sections throughout the Project area and calibrated to thermistor data. Following completion of the 2D thermal models, results were used to create a three-dimensional (3D) block model for each of the three main areas of the Project:

- Tiriganiaq, F Zone, Pump and Wesmeg/Wesmeg-North deposits (Main Area)
- Discovery Area
- Tiriganiaq-Wolf Area

The 3D ground temperature blocks are intended to provide an overall view of the permafrost conditions with the Project areas. The methodology and results of the thermal modelling is presented in Golder (2022). Results of the thermal modelling indicated:

- Open taliks (defined by the 0-degree isotherm) are predicted to be present beneath portions of each of the following lakes near the proposed open pits and undergrounds: Lake B4, B5, B7, A6, A8, and CH6. The model results expand the list of lakes with potential open talik compared to what was estimated in the 2014 Freshwater Environment FEIS, where only the Meliadine lake, and Lakes A8, B7 and D7 were considered large enough to support open talik.
- Closed talik is interpreted below Lake D4 based on the 0-degree isotherm, which is different from what was interpreted in the 2020 thermal assessment (Golder 2021a). Predicted temperatures, however, suggest that the ground below the lake may not be fully frozen in consideration of the groundwater salinity, and that the lake may be connected to the regional groundwater flow system through the cryopeg zone. Cryopeg is interpreted to present between temperatures of 0 to -3 degrees Celsius (See Section 3.5.2).
- Updated thermal modelling results for the Main area indicate the base of permafrost (i.e., 0°C isotherm) is between 320 and 490 m below ground surface, with the interpreted depth dependent on the proximity of the location to nearby lakes. This represents an increase of about 60 m in permafrost depth compared to what was predicted in the 2020 thermal assessment (Golder 2021a). The permafrost depth range predicted in the models is also consistent with what has been measured by string GT21-75 and estimated based on legacy data from string M98-195, both located in the Main area to the north of Lake A8. The predicted permafrost depth range is also in agreement with the 2014 Permafrost Baseline Study, in which the depth of permafrost in the project area was estimated to be between 360 m and 495 m.



- For the Discovery area, the predicted maximum permafrost depth is approximately 400 m, similar to what was predicted in the 2020 thermal assessment (Golder 2021e).
- Based on permafrost depth limits and talik conditions predicted in this study, as well as locations and depths of open pits and underground structures included in the CAD file provided by Agnico Eagle (Agnico Eagle 2020), open pits in F Zone and Discovery, which vary in depth between 70 and 140 mbgs, will all be within permafrost. The Wesmeg North pit is planned to be about 130 m deep and is under a portion of Lake B5 where the models predict the existence of open talik, suggesting this pit would operate in unfrozen ground. The Wesmeg05 pit is planned to be about 120 m deep and is partially under the north side of Lake A8, where the models also predict the existence of open talik. Therefore, this pit could operate in partially unfrozen ground. The Pump04 pit is planned to be under the south side of lake A8 where the models predicted the existence of open talik. Therefore, the pit could operate in partially unfrozen ground.

### 3.5.2 Cryopeg Depth

Permafrost is defined as soil or rock where temperatures remain at or below 0°C for at least two consecutive years. The freezing temperature of water decreases when pressure and salinity increase. Consequently, within the permafrost unfrozen ground can be encountered at temperatures less than 0°C and in isolated pockets. These areas of unfrozen ground water above the base of the permafrost (0°C isotherm) are referred to as cryopeg.

Groundwater inflows to the mine are expected to be negligible until mining extends below the depth of the permanently frozen portion of the permafrost into the cryopeg. The depth at which these inflows may occur will depend on the thickness of the cryopeg, and the freezing point depression caused by the groundwater salinity.

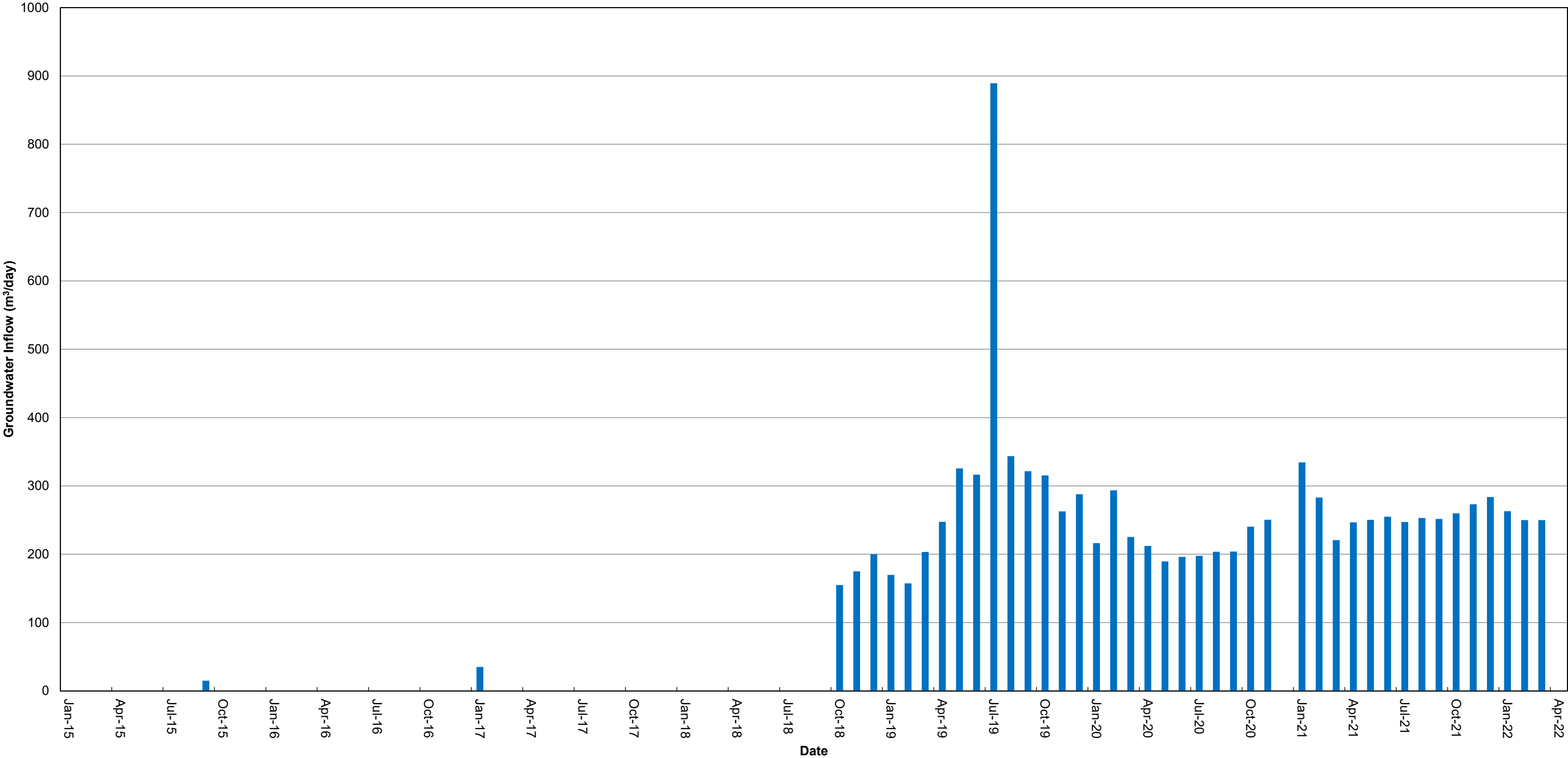
Deep groundwater samples collected near Tiriganiaq have a relative uniform TDS concentration of 55,000 mg/L. Considering the effect of salinity, the freezing point depression is therefore estimated to be approximately -3 degrees, and cryopeg conditions are assumed between the 0-degree and -3-degree isotherm. This may be somewhat conservatively adjacent to fresh-water lakes where groundwater salinity may be reduced, however, it is a conservative assumption for the assessment of groundwater inflows to underground developments. Near the Tiriganiaq underground away from the lakes, top of the cryopeg (base of the frozen permafrost) would be approximately 225 mbgs.

## 3.6 Tiriganiaq Groundwater Inflow Monitoring

Since the fourth quarter of 2015, groundwater inflow to the Tiriganiaq underground has been observed. Figure 7 presents a summary of groundwater inflow estimates based on sump measurements and seepage surveys for the Tiriganiaq Underground, as provided by Agnico Eagle. The groundwater inflow ranges from 15 m<sup>3</sup>/day in the fourth quarter of 2015, to more the recent 2021 and 2022 monthly inflow estimates of between 220 m<sup>3</sup>/day and 335 m<sup>3</sup>/day. Peak flows in 2019 and 2020 reflect periods where the boreholes were allowed to free drain into the underground as part of recession testing in the Tiriganiaq underground. Following completion of the testing and grouting of the boreholes, inflow to the underground decreased.

The observed inflow to the Tiriganiaq underground are thus far lower than the predicted inflows in the FEIS which ranged from 420 to 750 m<sup>3</sup>/day in the first few years of mining to 640 to 970 m<sup>3</sup>/day in later years. The lower than predicted inflows are to be expected because Agnico Eagle is mitigating the inflow of saline groundwater through active grouting as the development advances. Grouting was not considered in the FEIS groundwater inflow estimates.





CLIENT



CONSULTANT



YYYY-MM-DD 2021-05-25

PREPARED HG

DESIGNED HG

REVIEWED JL

APPROVED DC

PROJECT

AGNICO EAGLE MINES LIMITED  
MELIADINE EXTENSION  
NUNAVUT

TITLE

**GROUNDWATER INFLOW MEASUREMENTS  
FOR THE TIRIGANIAQ UNDERGROUND**

PROJECT NO.  
22513890

PHASE  
2000

REV.  
0

FIGURE  
7

### 3.7 Hydraulic Head Monitoring

#### 3.7.1 Tiriganiaq Area

Hydraulic head monitoring was conducted at Westbay Well M11-1257 as part of groundwater sampling, located to the south of Lake B7 and near Lake B5, and at several vibrating wire piezometers installed in the Tiriganiaq underground area to monitor depressurization during mining. The pressure recorded at each vibrating wire sensor was converted to equivalent fresh water hydraulic according to the following equation:

$$P = \rho_{fw} * g * H_{fw}$$

$$H_{fw} = \frac{P}{\rho_{fw} * g}$$

Where P is the pressure measured at the sensor,  $\rho_{fw}$  is density of freshwater (1000 kg/m<sup>3</sup>), g is the gravitation constant (9.8 m/s<sup>2</sup>) and  $H_{fw}$  is the equivalent freshwater hydraulic head.

As part of the FEIS, the approximate direction of groundwater flow between Lake B7 and M11-1257 was estimated using the freshwater heads with a correction for the buoyancy effects, as outlined by Post et al. (2007). These calculations are sensitive on the assumed TDS vs depth profile. For the assumed base TDS profile in the FEIS, which is overall consistent with the updated TDS profile presented in Section 3.4.2, the gradients for the individual ports and Lake B7 are variable but the overall groundwater flow direction between the lake and deep bedrock is downward.

**Table 12: Estimated Freshwater Heads, Flow Directions and Gradients – M11-1257 and Lake B7**

Borehole	Port	Vertical Depth (m)	Freshwater Head at Port (masl)	Freshwater Head at Lake B7 (masl)	Average Density (kg/m <sup>3</sup> )	Gradient
M11-1257	2	602.2	65.6	62	1023	0.0174
M11-1257	3	573.7	72	62	1022	0.0047
M11-1257	4	518.7	64.3	62	1020	0.0152
M11-1257	5	448.6	71.5	62	1015	-0.0058
Average Gradient						0.0079

Note: Gradients calculated between each multi-level port and Lake B7. A positive value indicates a downward gradient. Vertical depths are approximate, due to borehole deviation the actual depth could be +/- 1 m from the tabulated value.

M11-1257 is near Lake B5, which since the FEIS has been interpreted to have open talik below it. Table 13 presents the estimated freshwater heads, flow directions and gradients between M11-1257 and Lake B5. The direction of the vertical gradient between M11-1257 ports and Lake B5 is similar to the vertical gradients calculated between M11-1257 and Lake B7. An upward gradient is estimated to be present between the shallowest port (Port 5) and Lake B5 and a downward gradient is estimated to be present between the deeper ports (Ports 2, 3, and 4) and Lake B5.

**Table 13: Estimated Freshwater Heads, Flow Directions and Gradients - M11-1257 and Lake B5**

Borehole	Port	Vertical Depth (m)	Port Elevation (masl)	Freshwater Head at Port (masl)	Freshwater Head at Lake B5 (masl)	Average Density (kg/m <sup>3</sup> )	Gradient Between B5 and Port
M11-1257	2	602.2	-544.2	65.6	58	1028	0.016
M11-1257	3	573.7	-515.7	72.0	58	1028	0.003
M11-1257	4	518.7	-460.7	64.3	58	1026	0.014
M11-1257	5	448.6	-390.6	71.5	58	1023	-0.007

Note: Gradients calculated between each multi-level port and Lake B7. A positive value indicates a downward gradient.

Vibrating wire piezometers have been installed from the Tiriganiaq underground to measure changes in hydraulic head as mining progresses, as presented on Figure 8 to Figure 11. The measurements show high variability as result of intersection of permeable features, progressive grouting of the underground development, delays in grouting or sealing of vibrating wire piezometer in the borehole, and challenges / potential malfunction of the dataloggers. Although local temporal variations are difficult to understand in the piezometric data because of the multiple sources of this variability, the long-term trend of these data can be used to understand the extent of depressurization near the underground, particularly at sensors that were installed at the end of 2015, just after the underground extended into the cryopeg.

The data presented on Figure 8 indicates that depressurization has increased in the underground area as the mine development has advanced. Hydraulic heads are generally near the top of the cryopeg and indicate that saturated conditions are generally present near the underground development within the cryopeg and underlying bedrock.

### 3.7.2 Discovery Area

Pressure measurements at M20-3071 were recorded in 2021 prior to sampling and development efforts to evaluate the vertical hydraulic gradients between Lake CH6 and the sampling ports (Golder 2023). The approximate direction of vertical groundwater flow can be estimated using the freshwater heads with a correction for the buoyancy effects, as outlined in Post et al. (2007). If the TDS profile developed for the Project is assumed to calculate the average density between the lake and sampling port, the overall groundwater flow direction below Lake CH6 appears to be upwards (Table 14), suggesting groundwater is discharging to Lake CH6. At deep depths the interpreted gradient reverses, potentially because of the higher salinity groundwater at depth. The calculated directions of groundwater flow are approximate and sensitive to the assumed TDS versus depth profile. If the TDS at depth is assumed to trend to a lower value at depth (approximately 54,000 mg/L), a consistent upward gradient would be measured between each of the ports and Lake CH6.

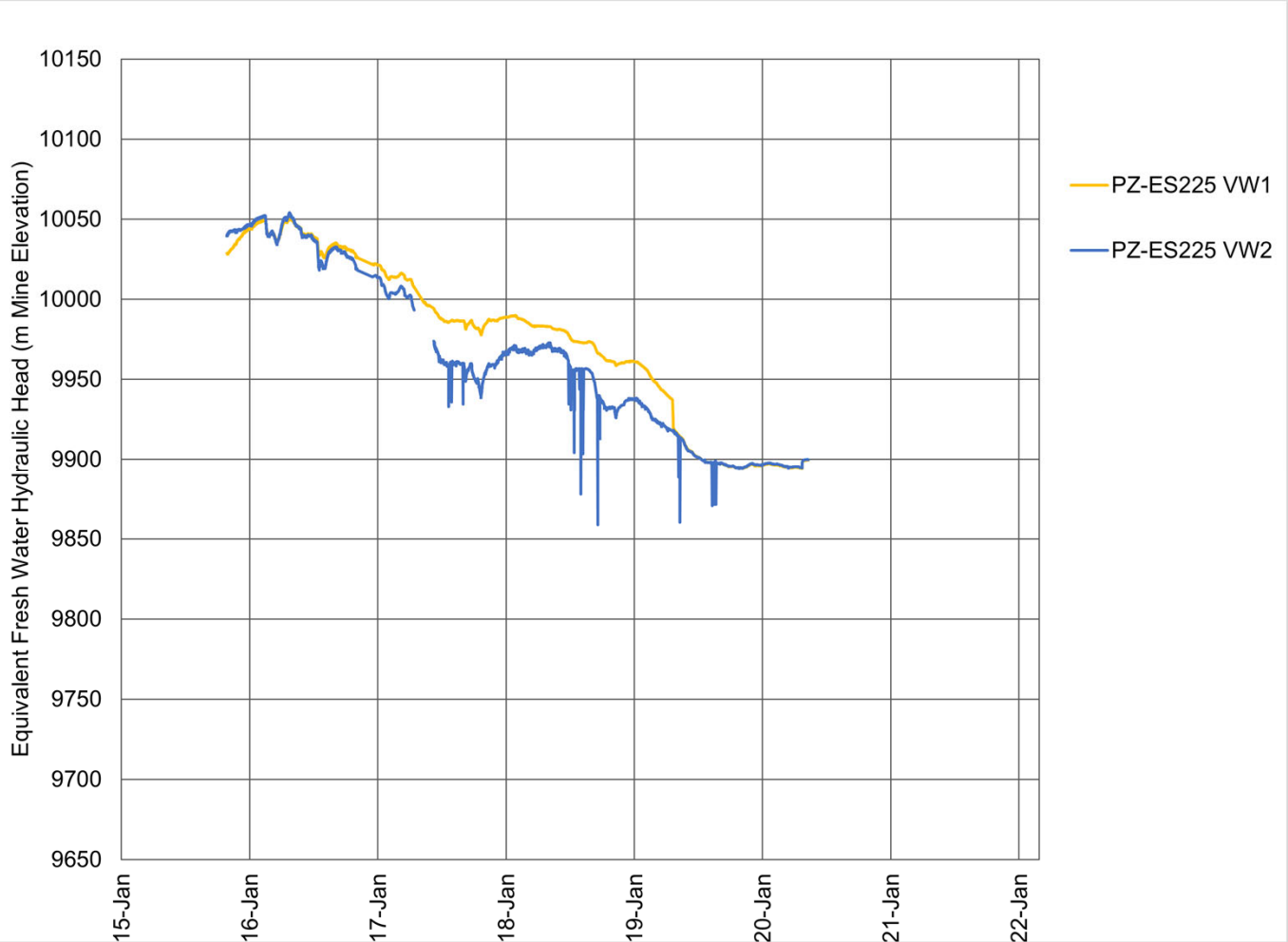
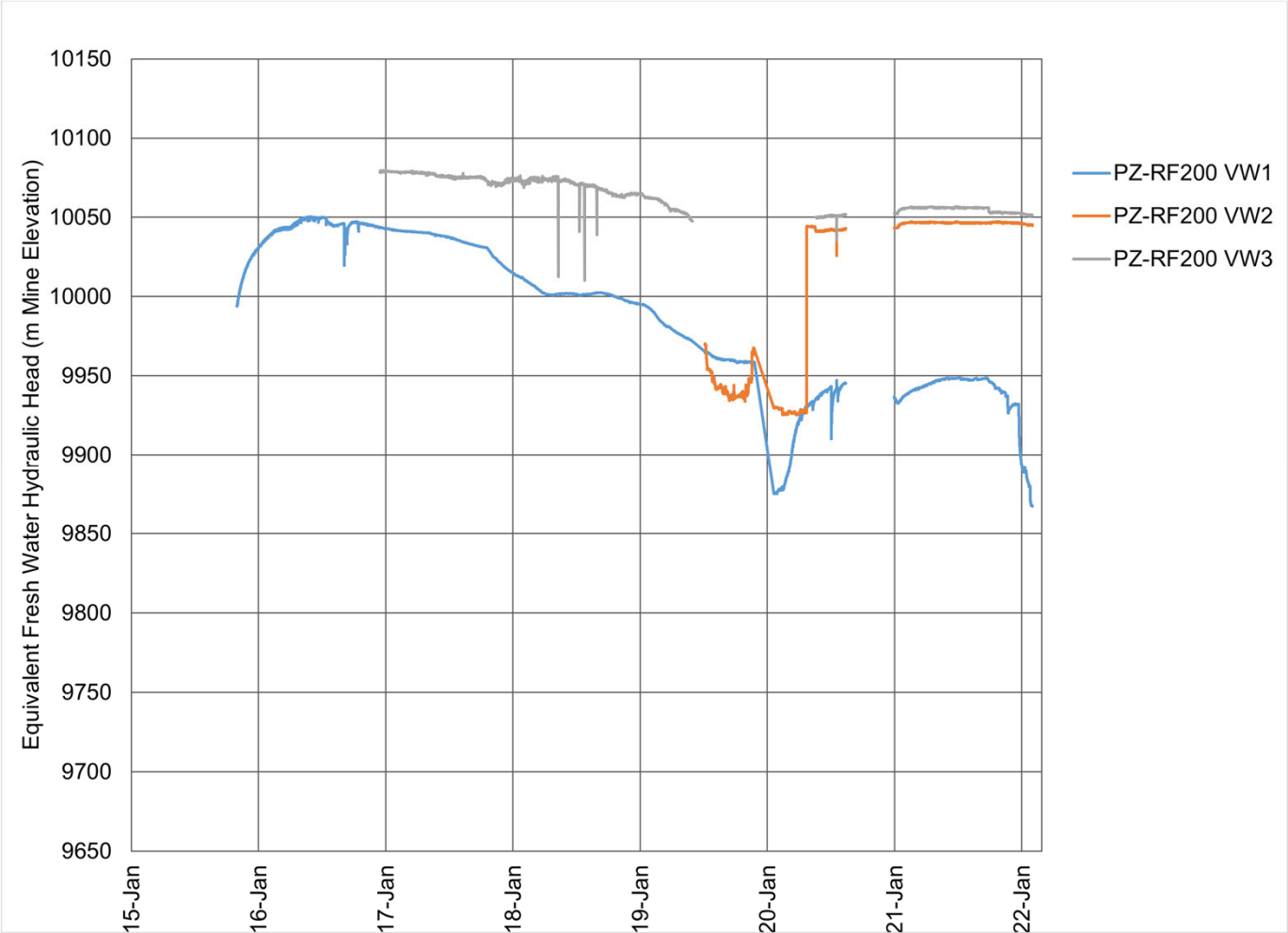
**Table 14: Estimated Freshwater Hydraulic Heads and Vertical Hydraulic Gradients**

Port	Port Position (masl)	Freshwater Head at Port (masl)	Freshwater Head at Lake CH6 (masl)	Average Density (kg/m <sup>3</sup> )	Gradient
11	-174.8	68.1	64	1,016	-0.008
10	-206.0	68.8	64	1,018	-0.006
9	-224.3	69.5	64	1,019	-0.006
8	-242.7	69.8	64	1,020	-0.004
7	-259.5	71.0	64	1,021	-0.006
6	-315.2	70.1	64	1,024	0.005
5	-326.3	68.1	64	1,025	0.012
4	-370.5	71.6	64	1,023	0.003
3	-370.5	71.6	64	1,023	0.003
2	-463.2	75.8	64	1,026	0.001
1	-475.4	76.3	64	1,027	0.001

**Notes:**

masl = metres above sea level (elevation). Gradients calculated between each multi-level Port and Lake CH6.

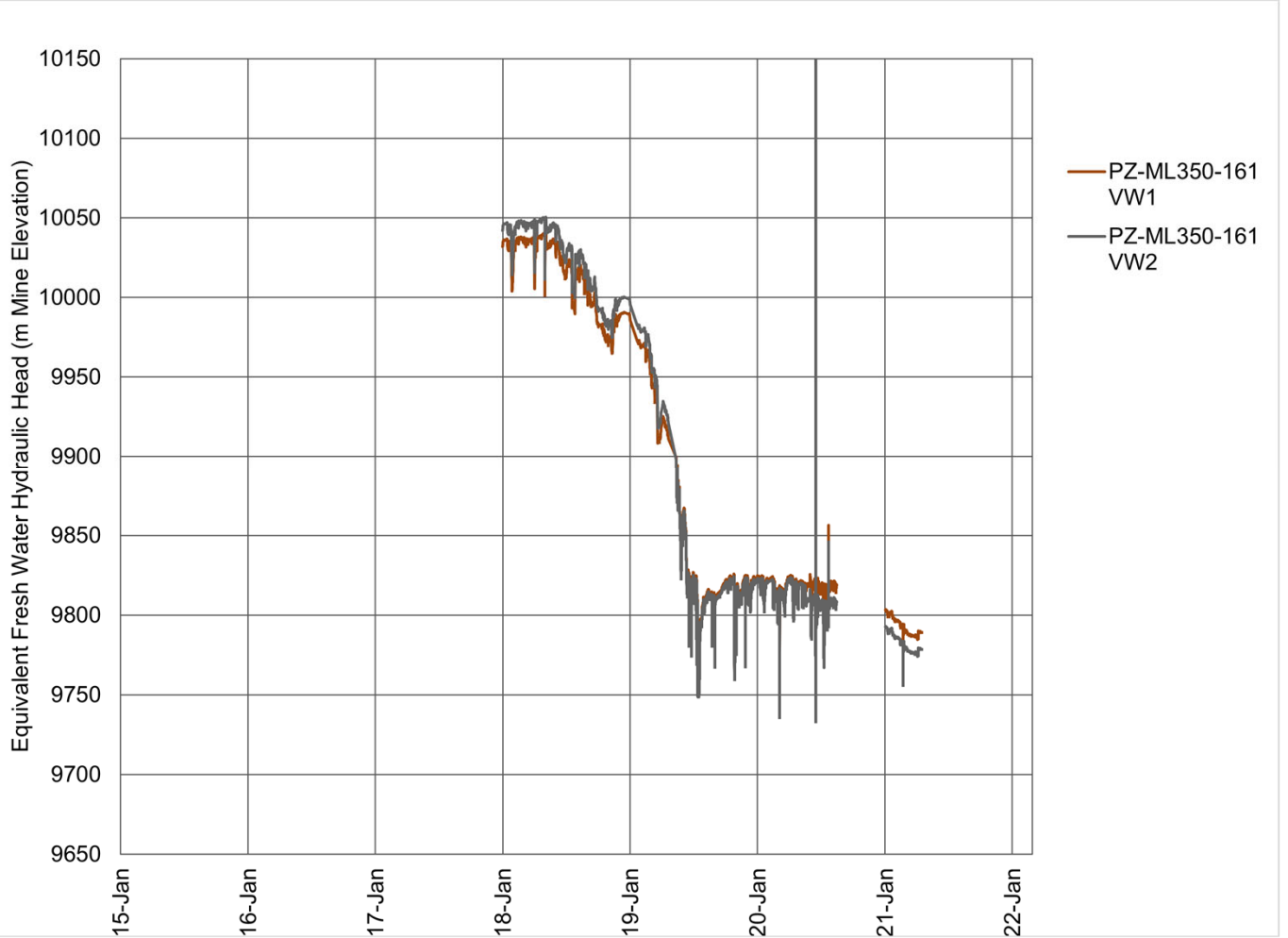
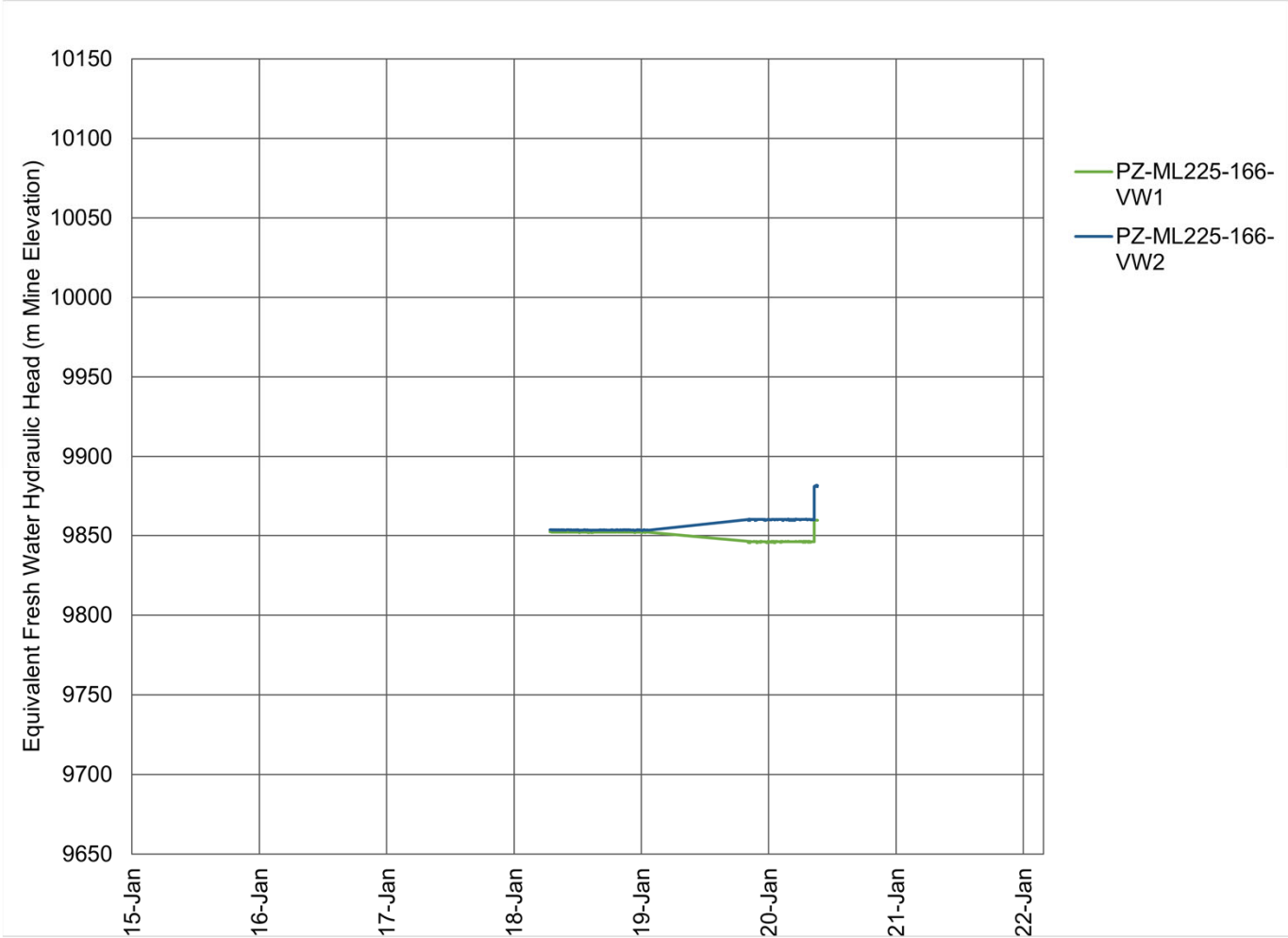
A positive value indicates a downward gradient. Port positions are approximate. Due to borehole deviation the actual elevations could be +/- 1 metre from the tabulated value.



Piezometer	Borehole ID	Node	Sensor Elevation (m Mine Grid)	Sensor Elevation (masl)	Approximate Sensor Depth (mbgs)	Hydrostratigraphic Unit
PZ-RF200-01	TIS-200-001	VW1	9729.3	-270.7	325.7	Volcanic Rock Formations
		VW2	9680.9	-319.1	374.1	Volcanic Rock Formations
		VW3	9435.3	-564.7	619.7	Volcanic Rock Formations
PZ-ES225-02	TIS-225-001	VW1	9726.8	-273.2	328.2	Volcanic Rock Formations
		VW2	9678.5	-321.5	376.5	Volcanic Rock Formations

As-Built Stage	Deepest Elevation of Mine (masl)	Deepest Elevation of Mine (m Mine Grid)
Q4 2015	-235	9765
Jun-16	-280	9720
Jun-17	-325	9675
Nov-18	-355	9645
Jan-19	-355	9645
Apr-20	-375	9625
Mar-22	-430	9570

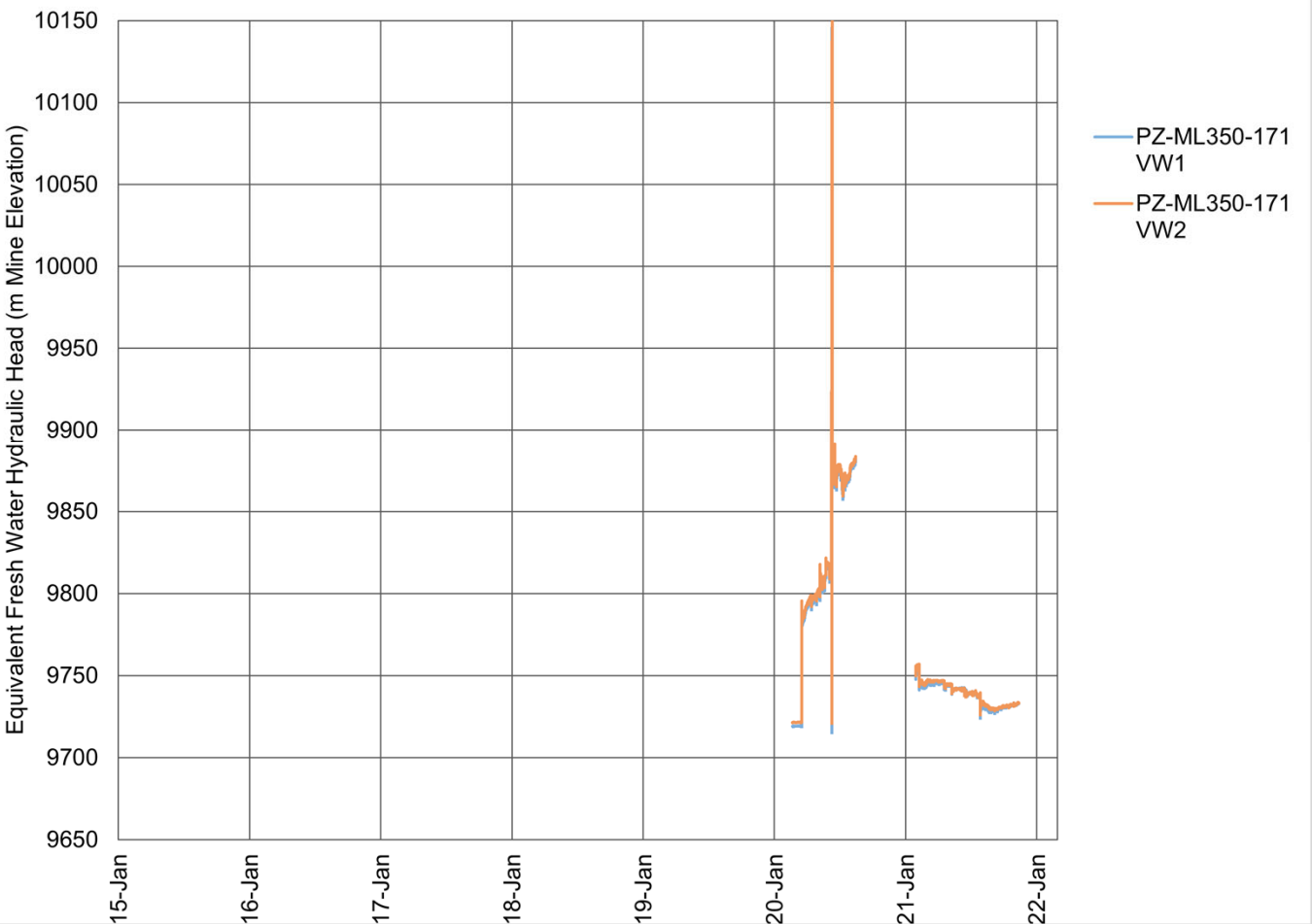
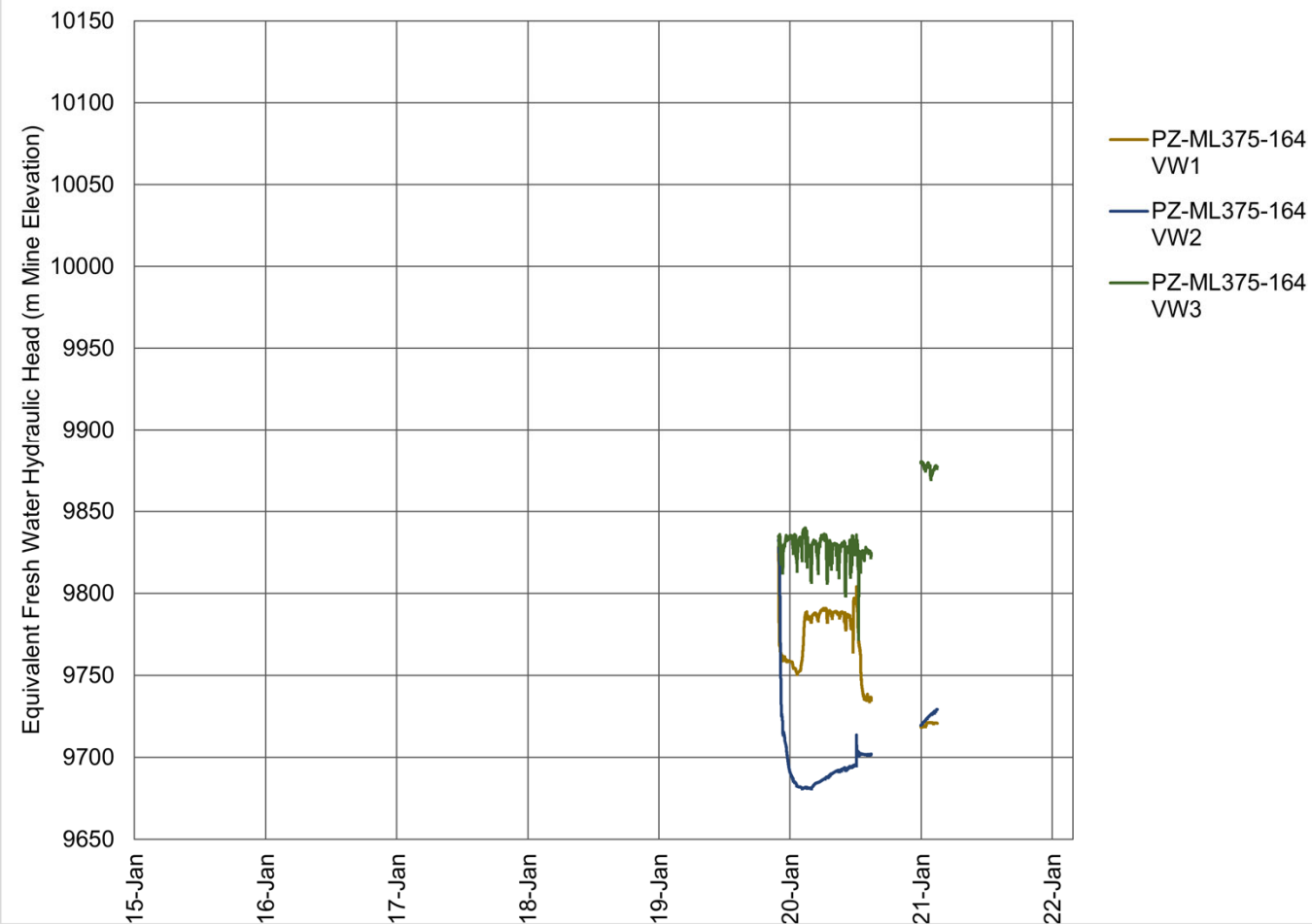
Note: Mine Grid Elevation is 10,000 m higher than Geodetic Elevation (masl).



Piezometer	Borehole ID	Node	Sensor Elevation (m Mine Grid)	Sensor Elevation (masl)	Approximate Sensor Depth (mbgs)	Hydrostratigraphic Unit
PZ-ML17-225-166	ML17-225-166-F1	VW1	9856.1	-143.9	198.9	Volcanic Rock Formations
		VW2	9856	-144	199.3	Lower Fault/KMS Corridor
PZ-ML17-350-161	ML17-350-161-001	VW1	9732	-268	323.4	Lower Fault/KMS Corridor
		VW2	9732	-268	323.2	Lower Fault/KMS Corridor

Note: Mine Grid Elevation is 10,000 m higher than Geodetic Elevation (masl).

As-Built Stage	Deepest Elevation of Mine (masl)	Deepest Elevation of Mine (m Mine Grid)
Q4 2015	-235	9765
Jun-16	-280	9720
Jun-17	-325	9675
Nov-18	-355	9645
Jan-19	-355	9645
Apr-20	-375	9625
Mar-22	-430	9570



Piezometer	Borehole ID	Node	Sensor Elevation (m Mine Grid)	Sensor Elevation (masl)	Approximate Sensor Depth (mbgs)	Hydrostratigraphic Unit
PZ-ML375-164	ML376-164-D1	VW1	9694	-306	361	Lower Fault/KMS Corridor
		VW2	9683	-317	372	Lower Fault/KMS Corridor
		VW3	9681	-319	374	Lower Fault/KMS Corridor
PZ-ML350-171	ML350-171-D1	VW1	9714	-286	341	Lower Fault/KMS Corridor
		VW2	9712	-288	343	Lower Fault/KMS Corridor

Note: Mine Grid Elevation is 10,000 m higher than Geodetic Elevation (masl).

As-Built Stage	Deepest Elevation of Mine (masl)	Deepest Elevation of Mine (m Mine Grid)
Q4 2015	-235	9765
Jun-16	-280	9720
Jun-17	-325	9675
Nov-18	-355	9645
Jan-19	-355	9645
Apr-20	-375	9625
Mar-22	-430	9570

CLIENT

CONSULTANT

PROJECT

AGNICO EAGLE MINES LIMITED  
MELIADINE EXTENSION  
NUNAVUT

TITLE

PRESSURE MONITORING DATA – TIRIGANIAQ UNDERGROUND – PART 3

PROJECT NO.

22513890

PHASE

2000

REV.

0

FIGURE

10

YYYY-MM-DD

2021-05-25

PREPARED

HG

DESIGNED

HG

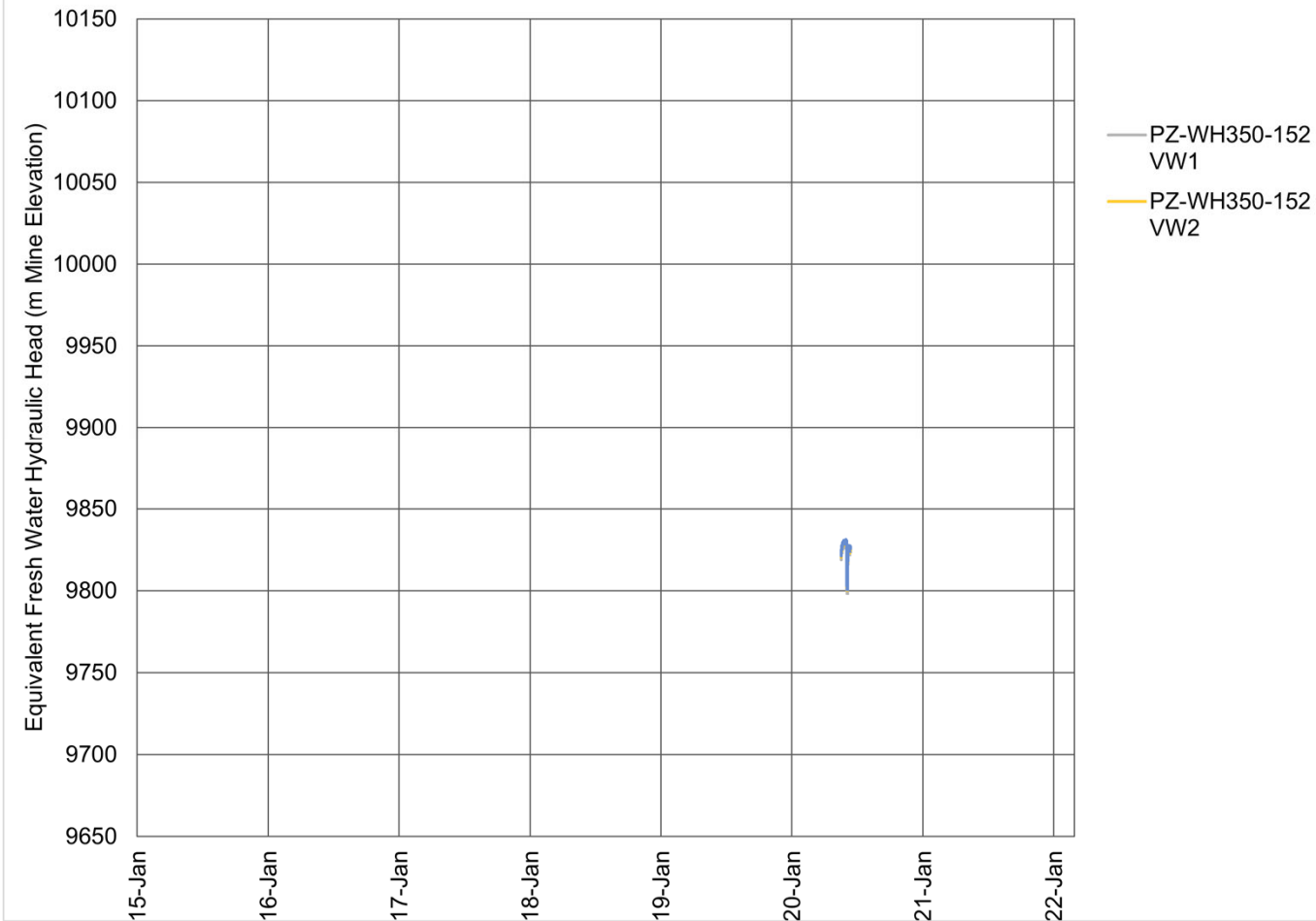
REVIEWED

JL

APPROVED

DC

IF THIS MEASUREMENT DOES NOT MATCH WHAT IS SHOWN, THE SHEET SIZE HAS BEEN MODIFIED FROM A3S-B



Piezometer	Borehole ID	Node	Sensor Elevation (m Mine Grid)	Sensor Elevation (masl)	Approximate Sensor Depth (mbgs)	Hydrostratigraphic Unit
PZ-WH350-152	WH350-152-D1	VW1	9724	-276	331	Lower Fault/KMS Corridor
		VW2	9720	-280	335	Lower Fault/KMS Corridor
		VW3	9715	-285	340	Sedimentary Rock Formations

Note: Mine Grid Elevation is 10,000 m higher than Geodetic Elevation (masl).

As-Built Stage	Deepest Elevation of Mine (masl)	Deepest Elevation of Mine (m Mine Grid)
Q4 2015	-235	9765
Jun-16	-280	9720
Jun-17	-325	9675
Nov-18	-355	9645
Jan-19	-355	9645
Apr-20	-375	9625
Mar-22	-430	9570

0 25mm IF THIS MEASUREMENT DOES NOT MATCH WHAT IS SHOWN, THE SHEET SIZE HAS BEEN MODIFIED FROM A3S-B



## 4.0 CONCEPTUAL HYDROGEOLOGICAL MODEL

Available hydrogeological data collected at the site, together with information collected elsewhere in the Canadian Shield, were used to develop a conceptual understanding of groundwater conditions at the Project. A conceptual hydrogeological model is a pictorial representation of the groundwater regime that organizes and simplifies the site hydrogeology so that it can be readily modelled. The conceptual model must retain sufficient complexity so that the analytical or numerical models developed from it adequately reproduce or simulate the actual components of the groundwater flow system to the degree necessary to satisfy the objectives of the modelling study. During the development of the conceptual model, the main hydrostratigraphic units are defined and characterized, and the dominant groundwater flow patterns are identified both prior to and during mine development. The hydrogeological conceptual model has been developed to describe key features of the hydrogeological regime. The key features include the permafrost depth, hydrostratigraphy/structural geology, groundwater quality, and groundwater flow, all of which are described in below. The baseline conceptual model is described below.

### 4.1 Permafrost Depth

The base of the permafrost is interpreted as an undulating surface that may vary with latitude, topography and proximity to taliks and it may vary spatially within the overall mine workings. Thermal modelling indicates the depth to permafrost varies between 320 and 490m depth, with the interpreted depth dependent on the proximity to nearby lakes. Based on the groundwater quality data for the Project (Section 3.4) and thermal modelling (Golder 2022a), the depth to the basal cryopeg where unfrozen groundwater may first be encountered near Tiriganiaq is expected to be approximately 300 mbgs.

Open taliks are present beneath portions of each of the following lakes near the proposed open pits and undergrounds: Lake B4, Lake B5, Lake B7, Lake A6, Lake A8, and Lake CH6. Closed talik is interpreted below Lake D4 based on the 0-degree isotherm, however the lake is interpreted to potentially connected to the regional groundwater flow system through the cryopeg zone. Based on permafrost limits, open pits in the F Zone, Pump and Discovery, which vary in depth between 70 and 140 mbgs, will be within permafrost. The Wesmeg-North pit is planned to be about 130 m deep and is under a portion of Lake B5 where the models predict the existence of an open talik. The Wesmeg05 pit is planned to be about 120 m deep and is partially under the north side of Lake A8, where the models also predict the existence of an open talik. Each of the underground developments extends into unfrozen bedrock and/or open talik below the lakes.

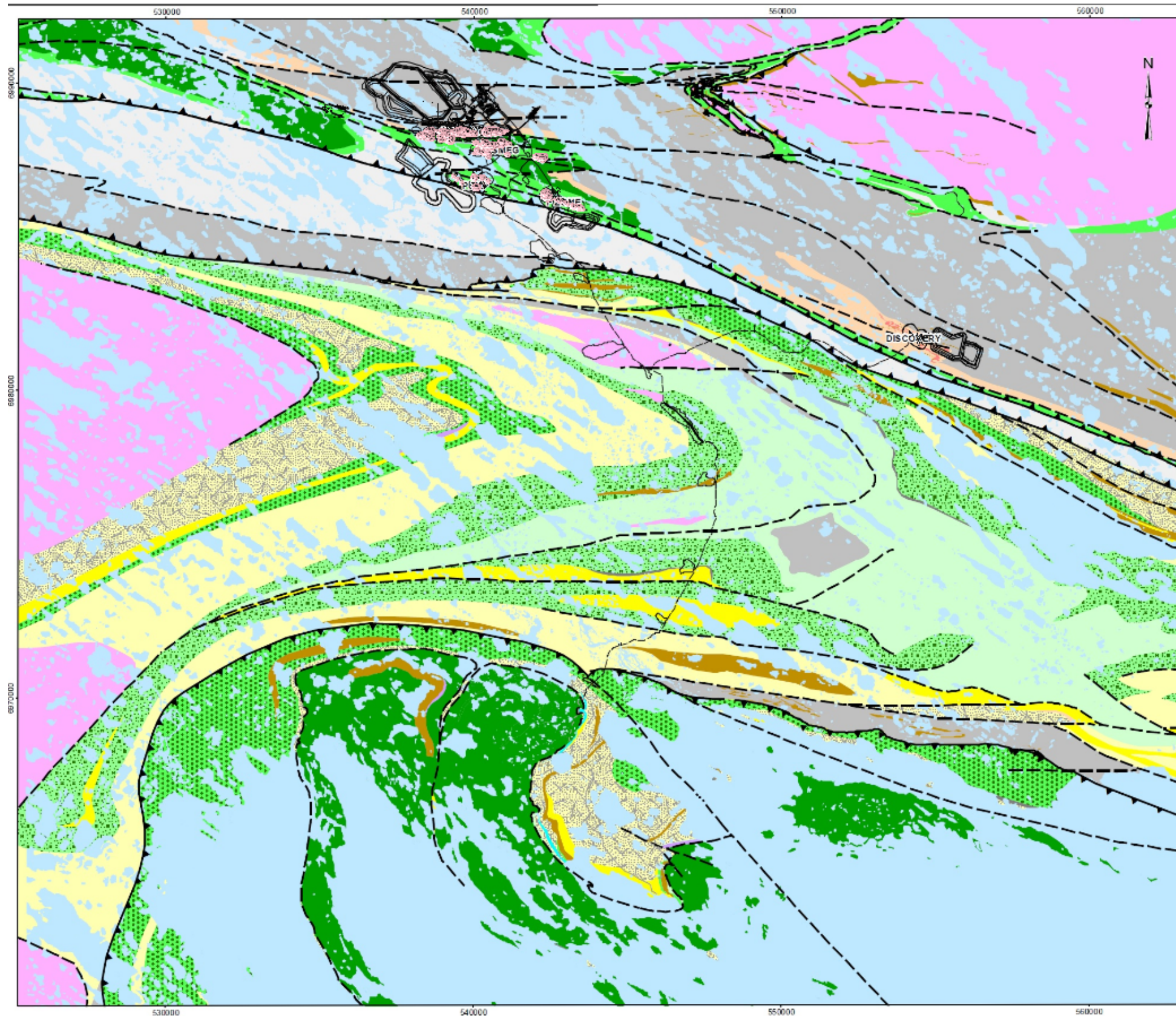
### 4.2 Hydrostratigraphy

#### 4.2.1 Geologic Context

The Project is located with the Archaean Rankin Inlet Greenstone Belt, within the Churchill Structural Province of the Canadian Shield (Figure 12). The rocks of the Rankin Inlet Greenstone Belt have been subjected to polyphase deformation events and metamorphism. The rocks consist of a sequence of mafic volcanic rocks, felsic pyroclastic rocks, sedimentary rocks and gabbro sills. The following descriptions are based on information contained in Snowden (2008) and Fingler (2001), as described in the 2014 FEIS (Agnico Eagle 2014a). For a more detailed description of the geology of the Project area, the reader is referred to these reports.

Archean and Proterozoic deformation events have resulted in an alignment of stratigraphy trending in a northwest to southeast direction which defines the Meliadine trend. To the south of the deposits is the Pyke Fault, a major regional fault zone, which extends over several kilometres and is characterized by multiple foliations and regional shear zones.





LEGEND

- Proposed Project Infrastructure
- All-weather Access Road (AWAR)
- Road - New
- Road - Existing
- Watercourse
- Waterbody
- Regional Geology
  - Quartzite
  - Quartzite-Siltstone
  - Pillowed Mafic Volcanic Rock
  - Quartzite-Felsic Volcanic Rock
  - Ultramafic Volcanic Rock
  - Greywacke-Iron Formation
  - Volcanic Rock
  - Mafic Volcanic Rock
  - Graywacke
  - Gabbro
  - Granitoid
  - Iron Formation
  - Andesitic Volcanic Rock
  - Carbonated Schist
  - Argillite
  - Conglomerate
  - Dolomite
  - Intermediate Volcanic Rock
  - Biotite Schist
- Major Fault

CLIENT



CONSULTANT



YYYY-MM-DD 2021-05-25

PREPARED HG

DESIGNED HG

REVIEWED JL

APPROVED DC

PROJECT

AGNICO EAGLE MINES LIMITED  
MELIADINE EXTENSION  
NUNAVUT

TITLE

REGIONAL GEOLOGY

PROJECT NO.  
22513890

PHASE  
2000

REV.  
0

FIGURE  
12



The geology of the Tiriganiaq Deposit consists of greywacke and argillite sediments (Sam Formation), iron formation, and mixed iron formation, greywacke, and siltstone (Upper Oxide Formation) in fault contact with underlying mafic volcanic rocks (Wesmeg Formation). The sequence tends in an east/west direction and dips northward at inclinations greater than about 60 degrees. The stratigraphy is aligned for over 3 km along the mineralized shear direction. The fault contact between the Tiriganiaq and the Wesmeg Formation is referred to as the Lower Fault Zone. A zone of graphitic, mineralized fault gouge (0.5 to 3 m in thickness) commonly occurs over this zone.

The stratigraphy of the F Zone area is dominated by mafic volcanic rocks and the east southeast striking Lower Lean Iron Formation. The deposit area is located north of the Pyke Fault that runs sub-parallel to the Lower Iron Formation. Mineralization of the F Zone is hosted by the Lower Lean Iron Formation and is associated with quartz veins and east striking shear zones.

The stratigraphy of the Discovery area is dominated by a thick package of inter-bedded clastic sedimentary units, chemical sediments (oxide facies iron formations) and minor gabbroic dikes. In the deposit area, the hanging wall to the main gold-bearing iron formation horizon is dominated by a greywacke unit which contains minor interbedded argillaceous units, chemical sediments, and gabbroic dikes. Gold mineralization is generally restricted to a folded and a variably sheared oxide facies iron formation package, which generally consists of banded chert and magnetite horizons with lesser interbedded chlorite-rich beds and chert and minor local interbedded greywacke units. The footwall to the main mineralized iron formation horizon consists of a similar succession of clastic sedimentary units as found in the hanging wall. The footwall stratigraphy is dominated by greywacke, with a more argillaceous interval, approximately 20 to 40 m below the mineralized iron formation.

There appears to be two parts to the Wesmeg gold deposit, a northern and southern part. In the northern part, the stratigraphy strikes east west and dips 65 degrees to the north. The stratigraphy in the southern part strikes northwest southeast and dips 50 degrees to the north. The host Wesmeg Formation is massive to pillowed basalts and interlayered mafic volcanoclastics, with rare gabbro dikes and some interflow sediments consisting of siltstone, mudstone, and minor iron formations.

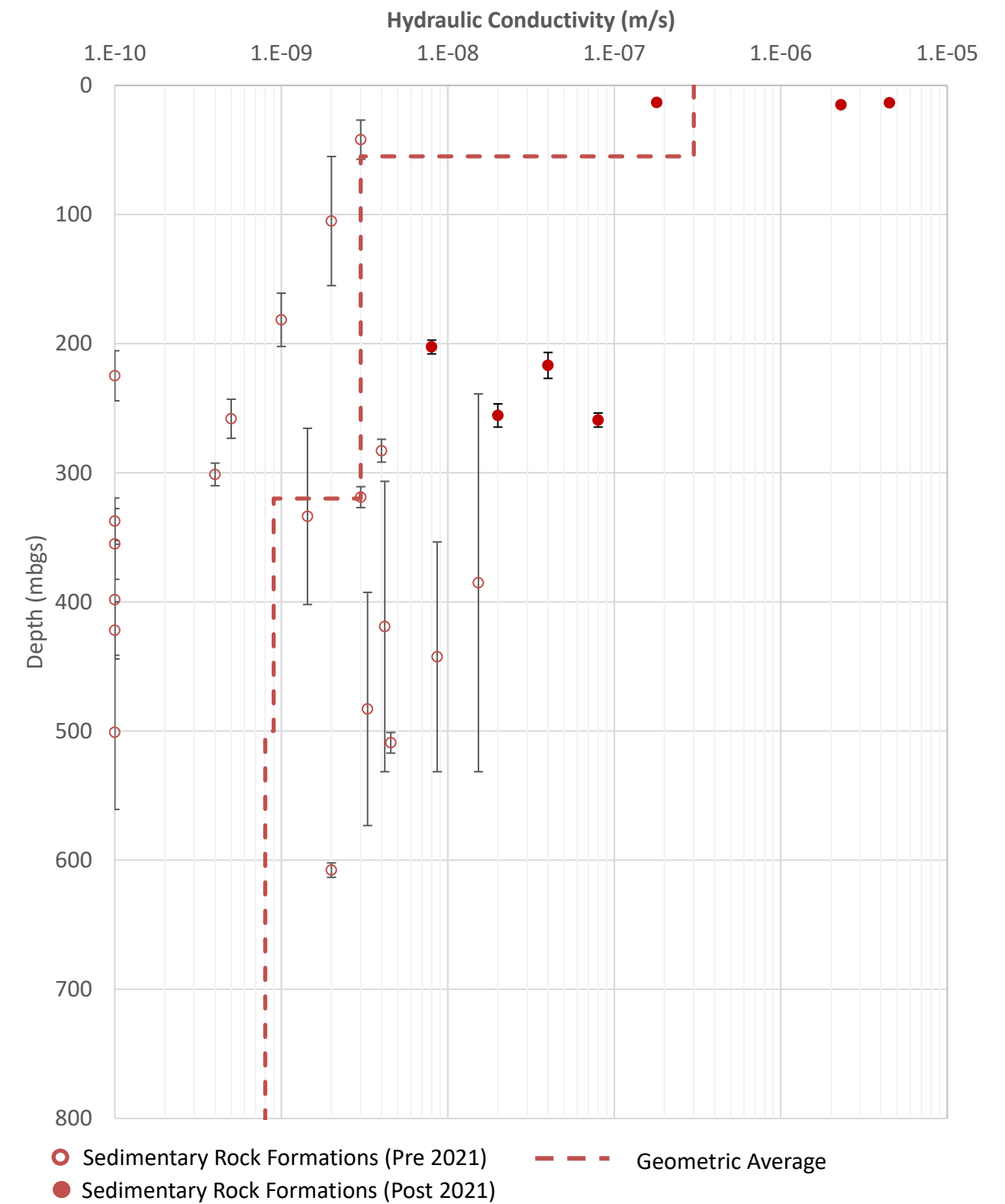
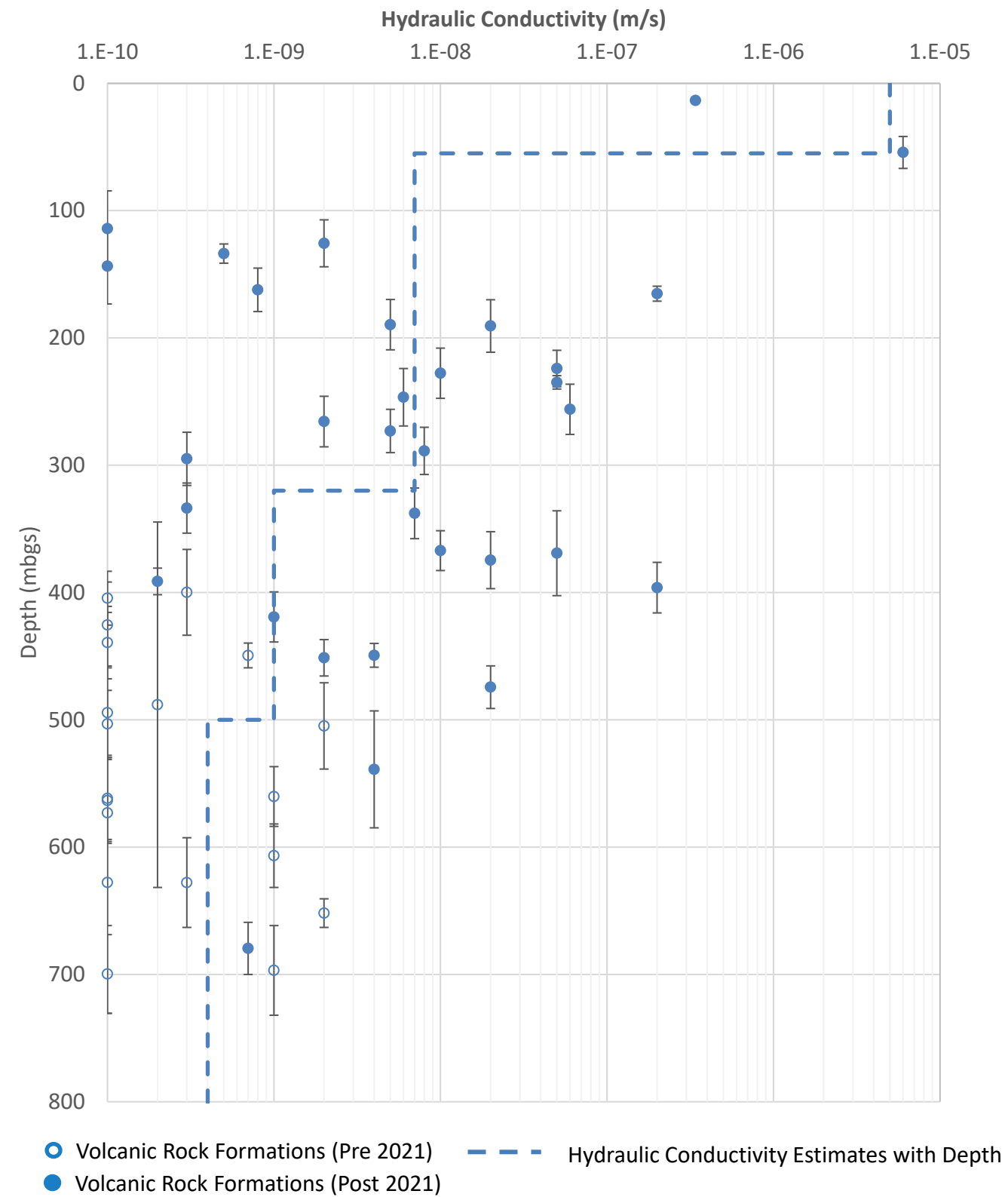
The stratigraphy in the Pump deposit are strikes northwest southeast and dips 50 degrees to the north. Like the F Zone and Wesmeg deposits, the host rocks at the Pump area are massive to pillowed basalts of the Wesmeg Formation, which are cut by rare gabbro dikes and interflow sediments.

## 4.2.2 Bedrock Hydrostratigraphy

The bedrock at the Meliadine Project was previously conceptualized as a single hydrostratigraphic unit (Agnico Eagle 2014a), with a near surface zone of higher hydraulic conductivity (shallow bedrock). The additional geological interpretation by Agnico Eagle since the 2014 FEIS has enabled a refined interpretation with additional data on the variability of hydraulic conductivity between geologic formations, and data on the storage properties of the bedrock. The current interpretation divides the competent bedrock into two separate units: Mafic Volcanic Rock formations and Sedimentary Rock formations. In past assessments, the Mafic Volcanic Rock Formations have been referred to as Footwall Unit, being in contact with the south side of the Lower Fault and includes the Wesmeg Formation. Agnico Eagle indicates the regional between the Lower Fault and Pyke Fault near Tiriganiaq, Tiriganiaq-Wolf, F Zone, Pump, Wesmeg and Wesmeg-North undergrounds is comprised of the Mafic Volcanic Rock formations. The Mafic rock transitions to Sedimentary Rock Formations towards the Discovery Underground and is also present to the north of the Lower Fault and south of the Pyke Fault, including the area near Tiriganiaq-Wolf and Tiriganiaq undergrounds. The Sedimentary Rock Formations have historically also been referred the Hanging Wall Unit, and contains the Sam, Upper Oxide and Tiriganiaq Formations.

Synthesis of the supplemental hydraulic testing results up to the end of 2021, supports previous interpretation that the Mafic Volcanic Rocks has lower hydraulic conductivity than the Sedimentary Rocks at depth. The supplemental data, however, show that the shallow and intermediate bedrock zones may be more permeable than the deeper bedrock. Figure 13 presents a summary of hydraulic conductivity test results collected to date and the calculated geometric averages from the updated data set.

Data presented in Figure 13 is representative of the hydraulic conductivity of the unfrozen rock. Consistent with the 2014 FEIS (Agnico Eagle 2014a) the hydraulic conductivity of the bedrock is assumed to be linearly reduced by an order of magnitude between the top of the basal cryopeg (isotherm of  $-3^{\circ}\text{C}$ ) and base of permafrost (isotherm of  $0^{\circ}\text{C}$ ). This assumption reflects that this portion of the permafrost, which will contain partially unfrozen groundwater due to freezing point depression, is expected to have reduced hydraulic conductivity relative to the unfrozen bedrock. The reduced hydraulic conductivity is attributed to the presence of isolated pockets of groundwater within this zone that may be frozen and that may result in a decrease in the hydraulic conductivity of the rock compared to that of the entirely unfrozen rock.



Note:  
1. Tests across fault intervals not shown.

CLIENT		PROJECT	
AGNICO EAGLE		AGNICO EAGLE MINES LIMITED MELIADINE EXTENSION NUNAVUT	
CONSULTANT		TITLE	
wsp GOLDER		SUMMARY OF AVAILABLE HYDRAULIC CONDUCTIVITY MEASUREMENTS – MAFIC VOLCANIC AND SEDIMENTARY ROCK FORMATIONS	
YYYY-MM-DD		2021-05-25	PROJECT NO.
PREPARED		HG	22513890
DESIGNED		HG	PHASE
REVIEWED		JL	2000
APPROVED		DC	REV.
			0
			FIGURE
			13

### 4.2.3 Enhanced Permeability Zones Associated with Faults

In crystalline rocks, fault zones may act as groundwater flow conduits, barriers, or a combination of the two in different regions of the fault depending on the direction of groundwater flow and the fault zone architecture (Gleeson and Novakowski 2009). In the 2014 FEIS, three regional structures were considered in hydrogeological assessment (Lower Fault, Pyke Fault and North Fault). In support of the Project, Agnico Eagle completed a review of the structures near the proposed underground developments through examination of more recent drilling data, magnetic surveys breaks and interpretation of surficial lineaments. This review led to the identification of 17 faults that have been incorporated into the conceptual hydrostratigraphy, in addition to the 3 regional faults (Lower Fault, Pyke Fault and North Fault) that were previously considered in the 2014 FEIS.

The following summarizes the conceptualization of faults within the Project area.

- **Lower Fault Zone** - The Lower Fault Zone that forms the fault contact between the Tiriganiaq and the Wesmeg formations, consists of a zone of strongly fractured graphitic and carbonized mudstones infilled with fault gouge in Tiriganiaq Underground. In the FEIS (Agnico Eagle 2014a), the Lower Fault Zone was assumed to be associated with enhanced permeability (hydraulic conductivity of  $1 \times 10^{-7}$  m/s) and to have a width of approximately 5 m. Observations made by Agnico Eagle during the advancement of the underground ramp in 2015 were consistent with this interpretation and suggested that the Lower Fault Zone is likely associated with enhanced permeability relative to the surrounding rock. Packer test estimates of hydraulic conductivity have ranged from  $5 \times 10^{-8}$  m/s to  $1 \times 10^{-7}$  m/s. From these measurements and the 2020 model calibration, the Lower Fault Zone is assumed to have a hydraulic conductivity of  $1 \times 10^{-7}$  m/s (See Section 4.2.4; Table 16).
- **North Fault** – The regional fault passing through the north end of Lake B7, referred to as the North Fault, has been assumed to have a hydraulic conductivity of  $1 \times 10^{-7}$  m/s and width of 5 m, consistent with the FEIS (Agnico Eagle 2014a) and previous groundwater modelling (Golder 2021). While present in the Project area, this fault does not intersect any of the proposed open pits or underground developments and is not interpreted to affect groundwater inflow to the underground developments. No site-specific measurements of hydraulic conductivity are available for the North Fault.
- **The Pyke Fault** – The Pyke fault is a larger (15 m wide) regional feature that extends through the Pump and F Zone undergrounds. Three tests have been conducted in two boreholes across the Pike Fault, with resulting estimated hydraulic conductivity values ranging between  $7 \times 10^{-9}$  to  $3 \times 10^{-7}$  m/s. The Pyke Fault hydraulic conductivity has been assumed equal to the upper bound of the packer test measurements.
- **KMS Corridor** – The KMS fault corridor is in the sedimentary rock formations to the north of the Lower Fault at the Tiriganiaq Underground. This corridor is a wider zone of rock located between the KMS fault and Lower Fault that is associated with poor rock quality. Assuming an average interpreted corridor thickness of approximately 100 m, the hydraulic conductivity of the corridor was estimated from flow recession testing and 2020 model calibration to be approximately  $4 \times 10^{-7}$  m/s. The flow recession data further indicated that the corridor has some compartmentalization and is not uniformly permeable throughout, as indicated by the calculated diffusivity values.

- **RM-175** – In the exploratory ramp, an enhanced permeability zone associated with the interpreted RM-175 was encountered. In the 2020 model, a hydraulic conductivity of  $5 \times 10^{-8}$  m/s was assigned to the RM-175 based on the observed inflow to the ramp from this structure and this value has been maintained in this updated assessment. The assumed value of  $5 \times 10^{-8}$  m/s is similar to but slightly higher than the estimate from packer testing at TIS-200-002 (Section 3.3).
- **Fault 2** – Fault 2 was estimated to have a hydraulic conductivity of  $1 \times 10^{-6}$  m/s based on the estimated packer test transmissivity of  $5 \times 10^{-6}$  m<sup>2</sup>/s and an observed fault width of 12 m. Supplemental 2021 testing has not been done in Fault 2, and the hydraulic conductivity is unchanged for this assessment.
- **Other Faults** – At the time of the 2020 groundwater model (Golder 2021g), limited testing had been conducted across other faults in the Project area. Considering the testing undertaken and potential variability across the length of each fault, each of the other faults were assumed to have a transmissivity of  $5 \times 10^{-6}$  m<sup>2</sup>/s, which was the maximum of the packer testing results over a fault excluding the KMS corridor. Supplemental testing has been conducted since the 2020 Model in Fault A, Fault 1, ENE1/ENE2, Fault C, and NW1 (Section 3.3). Transmissivity values from these tests have been lower than  $5 \times 10^{-6}$  m<sup>2</sup>/s, indicating the assumed hydraulic conductivity values for the other faults is likely conservatively high.

The lateral extents of the faults near the underground developments have not been mapped and therefore the faults have been conservatively extended approximately 2.5 km from intersected undergrounds. This is considered conservative since the permeability and width of a fault zone can be heterogeneous along strike (Gleeson and Novakowski 2009) resulting potentially in zones of greater hydraulic conductivity along strike over short distances; whereas over longer distances the presence of zones infilled with fault gouge will act to decrease hydraulic connectivity along strike. Observations during testing at Fault A is indicative of this variability.

#### 4.2.4 Estimated Hydraulic Properties

Table 15 and Table 15 present a summary of the hydrostratigraphic units and their estimated hydraulic properties based on the hydraulic testing presented in this report, past model calibration and based on published data for similar lithologies. These values will represent starting values for updated calibration of the numerical groundwater model.

Rational for the selected hydraulic conductivity for the competent bedrock is described below. Rational for selected hydraulic conductivity for the faults is presented in Section 4.2.3:

- For the shallow bedrock, the hydraulic conductivity of the bedrock is estimated from the arithmetic average of five available test results in the upper 55 m of rock. Relative to the 2020 model (Golder 2021g), this increases the hydraulic conductivity of the bedrock from the previously assigned value of  $3 \times 10^{-7}$  m/s, which was not based on site specific data.
- Between 55 and 320 mbgs and 320 and 500 mbgs, three times the geometric average is assumed for the hydraulic conductivity of the Volcanic Rock formations. Relative to the 2020 model (Golder 2021g), this increases the hydraulic conductivity of the bedrock from the calibrated values of  $3 \times 10^{-10}$  m/s but reflects the higher test values obtained in the 2021 supplemental data collection. Below 500 mbgs, the calibrated value of  $3 \times 10^{-10}$  m/s from the 2020 model was assumed.



- The geometric averages calculated between 55 and 320 mbgs and 320 and 500 mbgs for the Sedimentary Rock formations are less than the Volcanic Rock formations. Since there was less data, however, the hydraulic conductivity of the Sedimentary Rock formations was assumed equal to the Volcanic Rock formation to be conservative. Below 500 mbgs, the calibrated value of  $3 \times 10^{-9}$  m/s from the 2020 model was applied.

**Table 15: Estimated Hydraulic Properties - Competent Bedrock**

Hydrostratigraphic Unit	Depth Interval (mbgs)	Hydraulic Conductivity <sup>(a)</sup> (m/s)	Specific Storage <sup>(b)</sup> (1/m)	Effective Porosity <sup>(c)</sup> (-)
Shallow Rock	0 to 55	$3 \times 10^{-6}$	$1 \times 10^{-6}$	0.001
Sedimentary Rock Formations(d)	55 to 320	$2 \times 10^{-8}$	$1 \times 10^{-6}$	0.001
	320 to 500	$3 \times 10^{-9}$	$1 \times 10^{-6}$	0.001
	550 to 1500	$3 \times 10^{-9}$	$2 \times 10^{-6}$	0.001
Mafic Volcanic Rock Formations(d)	55 to 320	$2 \times 10^{-8}$	$1 \times 10^{-6}$	0.001
	320 to 500	$3 \times 10^{-9}$	$1 \times 10^{-6}$	0.001
	550 to 1500	$3 \times 10^{-10}$	$2 \times 10^{-7}$	0.001

Note: Hydraulic conductivity within the unfrozen permafrost zone is assumed to be lower than in the deeper unfrozen rock. Linearly decreasing hydraulic conductivity with temperature is assumed within this zone with a full order of magnitude decrease assumed at the top of the basal cryopeg, and hydraulic conductivity equivalent to unfrozen rock at the bottom of the basal cryopeg.

a) Parameter values based on in situ testing.

b) Parameter values based on in situ testing and values documented in literature (Maidment 1992; Stober and Bucher 2007).

c) Values consistent with literature values (Guimerà J, Carrera J. 2000).

**Table 16: Estimated Hydraulic Properties – Enhanced Permeability Zones**

Hydrostratigraphic Unit	Depth Interval <sup>(e)</sup> (m)	Thickness <sup>(d)</sup> (m)	Packer Test Hydraulic Conductivity Estimates (m/s)	# of Tests	Assumed Hydraulic Conductivity <sup>(a)</sup> (m/s)	Specific Storage <sup>(b)</sup> (1/m)	Effective Porosity <sup>(c)</sup> (-)	Source of Assigned Hydraulic Conductivity
Lower Fault Zone	0 to 1000	5	$5 \times 10^{-8}$ to $1 \times 10^{-7}$	4	$1 \times 10^{-7}$	$2 \times 10^{-7}$	0.001	2020 Model Calibration and In Situ Testing
RM-175	0 to 1000	5	$2 \times 10^{-8}$	1	$5 \times 10^{-8}$	$2 \times 10^{-7}$	0.001	2020 Model Calibration and In Situ Testing
KMS Fault Corridor	0 to 1000	100	$4 \times 10^{-7}$	1*	$4 \times 10^{-7}$	$2 \times 10^{-7}$	0.001	2020 Model Calibration and In Situ Testing
North Fault	0 to 1000	5	-	-	$1 \times 10^{-7}$	$2 \times 10^{-7}$	0.001	Unchanged from FEIS Assumption
A	0 to 1000	6	$2 \times 10^{-8}$ to $2 \times 10^{-7}$	6	$1 \times 10^{-6}$	$2 \times 10^{-7}$	0.001	Assumed T Equal to Fault 2 and In Situ Testing
B	0 to 1000	5	-	-	$1 \times 10^{-6}$	$2 \times 10^{-7}$	0.001	Assumed T Equal to Fault 2
C	0 to 1000	3	$4 \times 10^{-9}$	1	$2 \times 10^{-6}$	$2 \times 10^{-7}$	0.001	Assumed T Equal to Fault 2
D	0 to 1000	5	-	-	$1 \times 10^{-6}$	$2 \times 10^{-7}$	0.001	Assumed T Equal to Fault 2
Pyke Fault	0 to 1000	15	$7 \times 10^{-9}$ to $3 \times 10^{-7}$	3	$3 \times 10^{-7}$	$2 \times 10^{-7}$	0.001	Maximum from In Situ Testing
AP0	0 to 1000	3	-	-	$2 \times 10^{-6}$	$2 \times 10^{-7}$	0.001	Assumed T Equal to Fault 2
ENE1/ENE2	0 to 1000	5	$3 \times 10^{-8}$	1	$1 \times 10^{-6}$	$2 \times 10^{-7}$	0.001	Assumed T Equal to Fault 2
ENE3	0 to 1000	3	-	-	$2 \times 10^{-6}$	$2 \times 10^{-7}$	0.001	Assumed T Equal to Fault 2
UM2	0 to 1000	6	-	-	$1 \times 10^{-6}$	$2 \times 10^{-7}$	0.001	Assumed T Equal to Fault 2
NW1	0 to 1000	5	$2 \times 10^{-10}$ to $2 \times 10^{-9}$	3	$5 \times 10^{-7}$	$1 \times 10^{-7}$	0.001	Assumed T Equal to Fault 2
WNW1	0 to 1000	3	-	-	$2 \times 10^{-6}$	$2 \times 10^{-7}$	0.001	Assumed T Equal to Fault 2
WNW2	0 to 1000	3	-	-	$2 \times 10^{-6}$	$2 \times 10^{-7}$	0.001	Assumed T Equal to Fault 2
UAU2	0 to 1000	2	-	-	$3 \times 10^{-6}$	$2 \times 10^{-7}$	0.001	Assumed T Equal to Fault 2
Fault 1	0 to 1000	5	$8 \times 10^{-7}$	1	$1 \times 10^{-6}$	$2 \times 10^{-7}$	0.001	Assumed T Equal to Fault 2
Fault 2	0 to 1000	5	$3 \times 10^{-7}$ m/s and $5 \times 10^{-7}$	4	$1 \times 10^{-6}$	$2 \times 10^{-7}$	0.001	In Situ Testing
Fault 3	0 to 1000	5	-	-	$1 \times 10^{-6}$	$2 \times 10^{-7}$	0.001	Assumed T Equal to Fault 2

a) Hydraulic conductivity within the unfrozen permafrost zone is assumed to be lower than in the deeper unfrozen rock. Linearly decreasing hydraulic conductivity with temperature is assumed within this zone with a full order of magnitude decrease assumed at the top of the basal cryopeg, and hydraulic conductivity equivalent to unfrozen rock at the bottom of the basal cryopeg.

b) Assumed parameter in consideration of competent bedrock testing.

c) Values consistent with literature values (Guimerà J, Carrera J. 2000).

d) Width of structures estimated by Agnico Eagle from review of borehole records.

e) Where fault hydraulic conductivity is less than shallow rock, the fault was excluded from 0 to 60 m depth interval. Where fault hydraulic conductivity is greater than shallow rock, fault was included within 0 to 60 m depth interval.

### 4.3 Conceptual Groundwater Flow – Pre-Mining

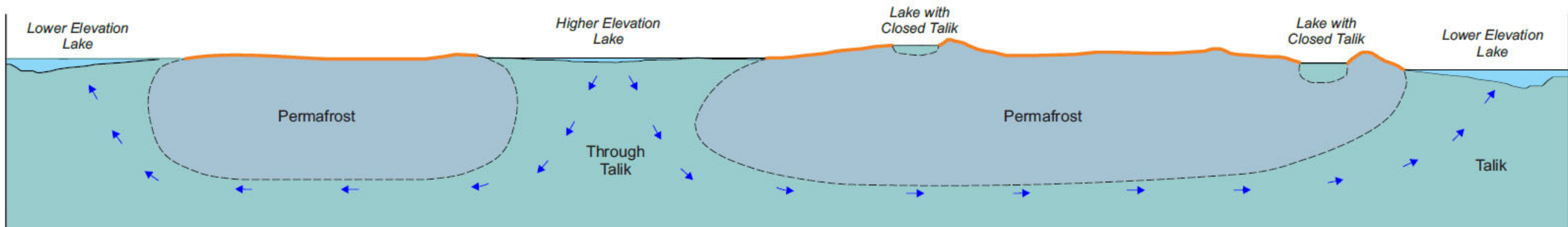
The conceptual hydrogeological model for pre-disturbance conditions is presented in Figure 14, with interpreted regional flow directions presented on Figure 1. In areas of continuous permafrost there are generally two groundwater flow regimes; a deep groundwater flow regime beneath the base of the permafrost and a shallow flow regime located in an active (seasonally thawed) layer near ground surface. Permafrost reduces the hydraulic conductivity of the rock by several orders of magnitude (McCauley et al. 2002; Burt and Williams 1976).

The shallow groundwater flow regime, therefore, has little to no hydraulic connection with the groundwater regime located below the permafrost. Taliks (areas of unfrozen ground surrounded by permafrost) may be present in the permafrost in areas underlying lakes. Depending on lake size, depth, and thermal storage capacity, the taliks beneath lakes may fully penetrate the permafrost layer resulting in an open talik providing a hydraulic connection between surface water and the deep groundwater flow regime.

The elevations of the lakes underlain by open taliks provide the driving force for deep groundwater flow. The presence of thick permafrost beneath land masses results in negligible recharge to the deep groundwater flow regime from these areas. Consequently, recharge to the deep groundwater flow regime is predominantly limited to areas of taliks beneath large, surface water bodies. Generally, deep groundwater will flow from higher-elevation lakes to lower-elevation lakes. Groundwater beneath the permafrost is also influenced by density differences due to the upward diffusion of deep-seated brines (density-driven flow).

The Westbay multi-level monitoring system that was installed in borehole M11-1257 is situated near Lake B5 between Lakes B7 and D7. Each of these lakes are predicted to be connected to the deep groundwater flow regime through open taliks. Relative to Lake B5, a variable vertical groundwater flow direction was observed at M11-1257. This may reflect that Lake B5 is both a recharge and discharge boundary given the relative elevation of the surrounding lakes.

The Westbay multi-level monitoring system that was installed in borehole M20-3071 is situated below Lake CH6. The overall groundwater flow direction below Lake CH6 appears to be upwards based on pressure measurements at M20-3071 corrected for buoyancy effects. At deeper depths the interpreted gradient reverses, potentially because of the higher salinity groundwater at depth. The calculated directions of groundwater flow are approximate and sensitive to the assumed TDS versus depth profile. For example, if the TDS at depth is assumed to trend to a lower value at depth (approximately 54,000 mg/L), a consistent upward gradient would be measured between each of the M20-3071 ports and Lake CH6.



CROSS SECTION

Schematic Only  
Not to Scale

LEGEND

- Conceptual Groundwater Flow Direction
- Active Layer

CLIENT			PROJECT			
AGNICO EAGLE			AGNICO EAGLE MINES LIMITED			
CONSULTANT			MELIADINE EXTENSION			
wsp GOLDER			NUNAVUT			
			TITLE			
			CONCEPTUAL PERMAFROST AND GROUNDWATER			
			FLOW MODEL – BASELINE CONDITIONS			
PROJECT NO.		22513890	PHASE		2000	REV.
						0
FIGURE		14				

## 4.4 Conceptual Groundwater Flow – Existing Conditions

Groundwater inflows are presently intercepted at the Tiriganiaq Underground, where mining has extended into the basal cryopeg and/or into the unfrozen rock below lakes with open taliks. In September of 2015, the mine development extended to the estimated depth of basal cryopeg and groundwater inflow was observed to the underground. Groundwater inflows were low (approximately 15 m<sup>3</sup>/day in the fourth quarter of 2015) but have since increased on an average of between 220 and 340 m<sup>3</sup>/day in 2021/2022. Groundwater inflows are mitigated by active grouting which locally reduces the effective hydraulic conductivity of structures adjacent to the development. At Tiriganiaq, local depressurization of over 450 m has been observed at piezometers installed near the underground. Further depressurization is expected at other undergrounds and open pits as they develop.

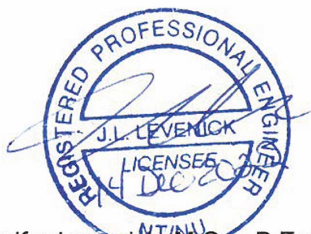
Each underground and open pit within the unfrozen rock will act as a sink for groundwater flow, with water induced to flow through the bedrock to the underground mine workings once the mine has advanced into and below the basal cryopeg, or into the open talik below a lake. These will include:

- Open Pits: Wesmeg-North, and Wesmeg05
- Undergrounds: Tiriganiaq, Tiriganiaq-Wolf, Pump, F Zone, Wesmeg, Wesmeg-North, Discovery

Outside of Wesmeg-North and Wesmeg05, none of the other open pits are interpreted to intersect the cryopeg or deep groundwater regime below the permafrost. Portions of the pits may intersect small layers and may have limited unfrozen groundwater within closed taliks.

## Signature Page

### Golder Associates Ltd.




Jennifer Levenick, M.Sc., P.Eng.  
*Principal, Senior Hydrogeologist*

A handwritten signature in blue ink, appearing to read "Don Chorley".

Don Chorley, M.Sc., P.Geo  
*Specialist Hydrogeologist*

JL/DC/anr

[https://golderassociates.sharepoint.com/sites/158318/project files/6 deliverables/01\\_issued/22513890-942-r-rev0-existing conditions/22513890-942-r-rev0-2000-existingconditions](https://golderassociates.sharepoint.com/sites/158318/project%20files/6%20deliverables/01_issued/22513890-942-r-rev0-existing%20conditions/22513890-942-r-rev0-2000-existingconditions)  
14dec\_22.docx

<p><b>PERMIT TO PRACTICE</b> <b>GOLDER ASSOCIATES LTD.</b></p> <p>Signature <u></u></p> <p>Date <u>2022-12-15</u></p> <p><b>PERMIT NUMBER: P 049</b> NT/NU Association of Professional Engineers and Geoscientists</p>
---

## REFERENCES

- Agnico Eagle (Agnico Eagle Ltd.). 2014a. Volume 7.0 Freshwater Environmental, Final Environmental Impact Statement (FEIS) – Meliadine Gold Project. Report Number Doc 314-1314280007 Ver. 0. April 2014
- Agnico Eagle. 2014b. Meliadine – Westbay Well 2014 Sampling Campaign. 22 July 2014.
- Agnico Eagle. 2014c. Follow-Up of Deep Ground Thermistor Cables at Meliadine – Compilation of the Data from 1998 to 2014. Revision A. October 2014.
- Agnico Eagle (Agnico Eagle Mines Ltd.). 2020. Option E\_PLOM2020\_final\_V4.dwg. CAD File provided by Agnico Eagle Mines Ltd.
- Blowes, D.W. and M.J. Logsdon. 1997. Diavik Geochemistry 1996-1997 Baseline Report. Prepared for Diavik Diamond Mines Inc.
- Burt, T.P. and P.J. Williams. 1976. Hydraulic Conductivity in Frozen Soils, Earth Surface Processes, Volume 1, John Wiley, pp. 349-360.
- Cumberland Resources Ltd., 2005. Meadowbank Gold Project Mine Waste and Water Management. October 2005.
- De Beers (De Beers Canada Inc.). 2010. Environmental Impact Statement for the Gahcho Kue Project. Volumes 1, 2, 3a, 3b, 4, 5, 6a, 6b, 7 and Annexes A through N. Submitted to Mackenzie Valley Environmental Impact Review Board. December 2010.
- Dominion Diamond (Dominion Diamond Ekati Corporation). 2014. Developer's Assessment Report Hydrogeology Baseline Report Annex IX. September 2014.
- Dyke, A.S., A. Moore, and L. Robertson. 2003. Deglaciation of North America, Geological Survey of Canada Open File 1574.
- Fingler, J.F. 2001. 2000 Geological, geochemical, geophysical and diamond drilling report for the Fay 1, Fay 2 and Felsic 1 Concessions, Meliadine East Property. NTI Assessment Report for Cumberland Resources Ltd. On behalf of the Meliadine East Joint Venture.
- Frape, S.K. and P. Fritz. 1987. Geochemical Trends for Groundwaters from the Canadian Shield; in Saline Water and Gases in Crystalline Rocks. Editors: Fritz, P. And Frape, S.K. Geological Association of Canada Special Paper 33.
- Gleeson, T. and K.S. Novakowski. 2009. Identifying watershed barriers to groundwater flow: Lineaments in the Canadian Shield. Geological Society of America Bulletin, 121:333-347.
- Golder (Golder Associates Ltd.). 2004. Predictions of Brackish Water Upwelling in Open Pits, Meadowbank Project Nunavut.
- Golder. 2009. Hydrogeologic Investigation Program – Meliadine Project. Doc. 039. Golder Associates Ltd. 6 November 2009.
- Golder. 2011. Appendix 7.2-C 2009 and 2011 Hydrogeological Testing and Groundwater Sampling Programs. Doc 436-1314280007 Ver 0



- Golder. 2014. SD 6-1 Permafrost Thermal Regime Baseline Studies – Meliadine Golder Project Nunavut. September 25 2012. Report Number: Doc 225-1013730076 Ver.0.
- Golder. 2016. Factual Report for Meliadine Project, Nunavut. Hydrogeological Investigation in Support of the Underground Mine Development at Tiriganiaq. Golder Doc. 547-1416135 Ver 0. 18 March 2016.
- Golder. 2021a. 2020 Hydrogeological Testing and Thermistor Installation Program. Golder Doc. 20136436-804-R-Rev0. May 2021.
- Golder. 2021b. Meliadine Extension – 2020 Thermal Assessment. Golder Doc. 20136436-815-R-Rev1. November 2021.
- Golder. 2021c. Westbay Monitoring Well System M20-3071 Groundwater Quality Assessment Meliadine Extension. Golder Doc. 20136436-817-R-Rev1. November 2021.
- Golder. 2021d. Installation of Westbay Monitoring Well System M20-3071 Meliadine Extension . Golder Doc. 20136436-820-R-Rev2. November 2021.
- Golder. 2021e. Results of Hydrogeological Testing in Wesmeg UG Borehole – Meliadine Phase II Project. Golder Doc 20136436-855-R-Rev0. December 2021
- Golder. 2021f. Summary of Hydrogeology Existing Conditions Meliadine Extension. Golder Doc. 20136436-855-R-Rev2. December 2021.
- Golder. 2021g. Hydrogeology Modelling Report Meliadine Extension. Golder Doc. 20136436-857-R-Rev3-2300.
- Golder. 2022. Meliadine Extension – 2021 Thermal Assessment. Golder Doc. 20136436-938-R-RevA. May 2022.
- Golder. 2022a. 2021 Hydrogeological Testing Program. Golder Doc. 20446358-893-R-Rev0. March 2021.
- Golder. 2022b. 2021 Discovery Hydrogeological Testing Program. Golder Doc. 20446358-888-R-Rev0.
- Golder. 2022c. Westbay Monitoring Well System M20-3071 2021 Groundwater Monitoring Program Meliadine Extension. Golder Doc. 21468783-911-R-Rev0
- Kuchling, K., D. Chorley and W. Zawadzki. 2000. Hydrogeological modelling of mining operations at the Diavik Diamonds Project. In Proceedings of the Sixth International Symposium on Environmental Issues and Waste Management in Energy and Mineral Production, University of Calgary, Calgary AB.
- McCauley, C.A, D.M. White, M.R. Lilly, and D.M. Nyman. 2002. A comparison of hydraulic conductivities, permeabilities and infiltration rates in frozen and unfrozen soils. Cold Regions Science and Technology 34(2002). PP. 117-125.
- Ophori, D.U., and Chan, T. 1994. Regional Groundwater Flow in the Atikokan Research Area; Simulation of 18O and 3H Distributions. AECL-11083. Manitoba.
- Post, B., Kooi, H. and Simmons, C., 2007. Using hydraulic head measurements in variable-density ground water flow analyses. Ground Water, 45(6): 664-671.
- R.L.&L. (R.L.&L. Environmental Services Ltd. 199. Meliadine West Baseline Aquatic Studies: 1988 Data Report. Prepared for WMC International Ltd.
- Séguin, A. 1995. Origin of saline groundwaters in Torbolton Ward, Eastern Ontario. Master of Science Thesis, Department of Earth Sciences, University of Ottawa, Ontario.

Snowden 2008. Comaplex Minerals Corp. Report on Tiriganiaq Gold Deposit, Nunavut – Resource Update January 2018. Stotler, R, S.K. Frape, T. Ruskeeniemi, P. Pitkänen, and D.W. Blowes. 2012. The interglacial–glacial cycle and geochemical evolution of Canadian and Fennoscandian Shield groundwaters. *Geochimica et Cosmochimica Acta* 76 (2012): 45–67.

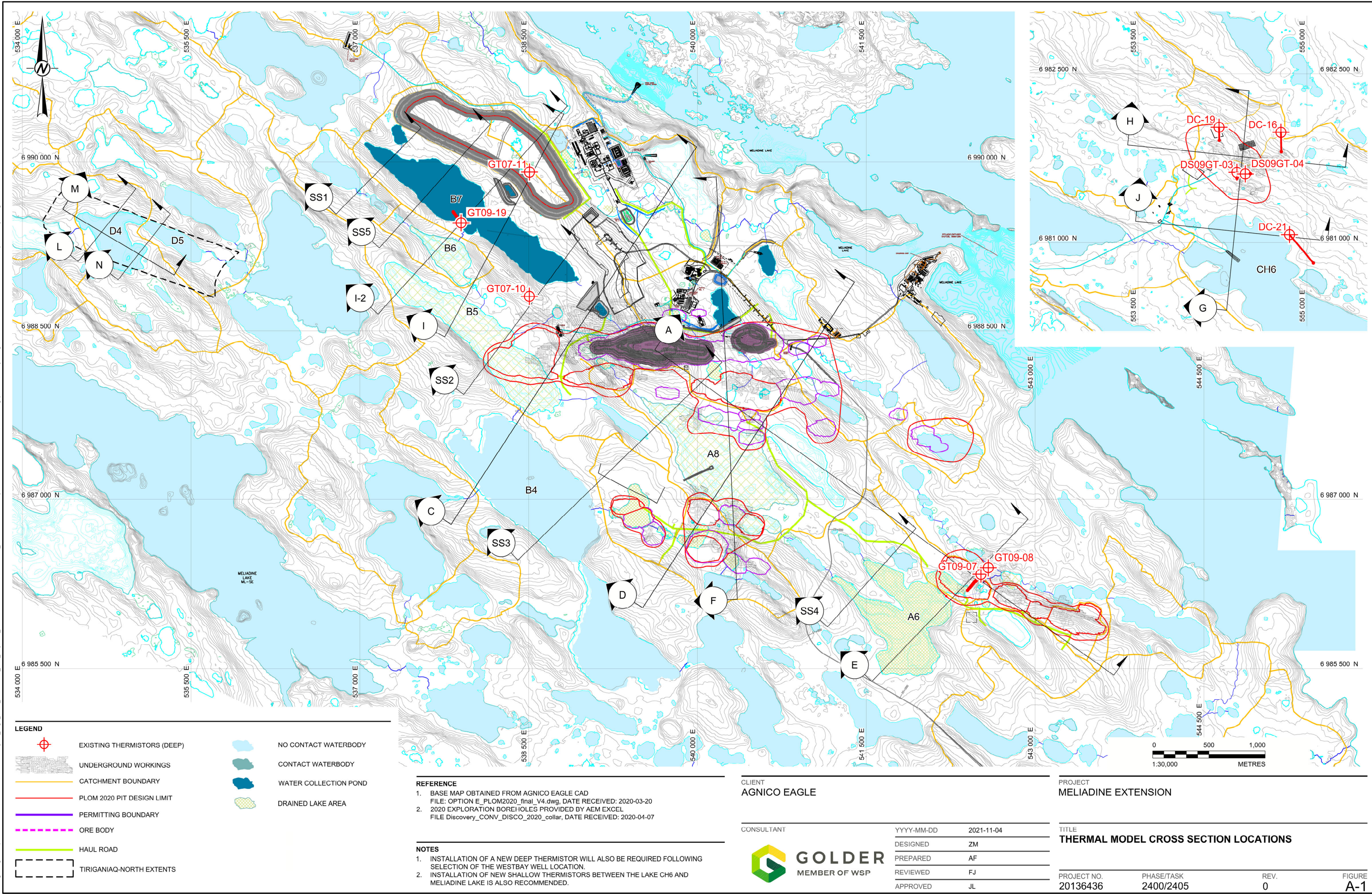
Tetra Tech. 2021. Spring 2021 Geotechnical Site Investigation, Meliadine Gold Project, NU. September 2021.

**APPENDIX A**

**Location of Thermal Model  
Cross-Sections**



Path: \\golder-gds-compl\data\office\Vanover\CAD-GIS\Client\Agnico\_Eagle\_Mines\_Ltd\Meliadine\_Gold\_Projects\03\_PROJECT\2021\3643624\02\05\02\_PRODUCTION\DWG | File Name: 2013643624\02\05\01.dwg | Last Edited By: amaghean Date: 2021-11-04 Time: 2:26:36 PM | Printed By: amaghean Date: 2021-11-05 Time: 8:42:33 AM







[golder.com](http://golder.com)